2006

Cyclicity in the nearshore marine to coastal, Lower Permian, Pebbley Beach Formation, southern Sydney Basin, Australia: a record of relative sea-level fluctuations at the close of the late Palaeozoic Gondwanan ice age

Brian G. Jones
University of Wollongong, briangj@uow.edu.au

Stuart C. Tye
Husky Energy, Calgary, CANADA

James A. Maceachern
Dept of Earth Sciences, Simon Fraser Uni, CANADA

Kerrie L. Bann
Ichnofacies PL, Calgary, CANADA

Christopher R. Fielding
Dept of Geosciences, Uni of Nebraska-Lincoln USA

Cyclicity in the nearshore marine to coastal, Lower Permian, Pebbley Beach Formation, southern Sydney Basin, Australia: a record of relative sea-level fluctuations at the close of the late Palaeozoic Gondwanan ice age

Abstract

The Lower Permian (Artinskian to Sakmarian) Pebbley Beach Formation of the southernmost Sydney Basin in New South Wales, Australia, records sediment accumulation in shallow marine to coastal environments at the close of the Late Palaeozoic Gondwanan ice age. This paper presents a sequence stratigraphic re-evaluation of the upper half of the unit based on the integration of sedimentology and ichnology. Ten facies are recognized, separated into two facies associations. Facies Association A (7 facies) comprises variably bioturbated siltstones and sandstones with marine body fossils, interpreted to record sediment accumulation in open marine environments ranging from lower offshore to middle shoreface water depths. Evidence of deltaic influence is seen in several Association A facies. Facies Association B (3 facies) comprises mainly heterolithic, interlaminated and thinly interbedded sandstone and siltstone with some thicker intervals of dark grey, organic-rich mudstone, some units clearly filling incised channel forms. These facies are interpreted as the deposits of estuarine channels and basins. Throughout the upper half of the formation, erosion surfaces with several metres relief abruptly separate open marine facies of Association A (below) from estuarine facies of Association B (above). Vertical facies changes imply significant basinward shift of environment across these surfaces, and lowering of relative sea level on the order of 50 metres. These surfaces can be traced over several kilometres along depositional strike, and are defined as sequence boundaries. On this basis, at least nine sequences have been recognized in the upper half of the formation, each of which is <10 m>thick, condensed, incomplete and top-truncated. Sequences contain little if any record of the lowstand systems tract, a more substantial transgressive systems tract and a highstand systems tract that is erosionally truncated (or in some cases, missing). This distinctive stacking pattern (which suggests a dominance of retrogradation and progradation over aggradation) and 3 the implied relative sea-level drop across sequence boundaries of tens of metres are remarkably similar to some other studies of continental margin successions formed under the Neogene icehouse climatic regime. Accordingly, it is suggested that the stratigraphic architecture of the Pebbley Beach Formation was a result of an Icehouse climate regime characterised by repeated, high-amplitude cycles of relative sea-level change.

Keywords

Cyclicity, nearshore, marine, coastal, Lower, Permian, Pebbley, Beach, Formation, southern, Sydney, Basin, Australia, record, relative, sea, level, fluctuations, close, late, Palaeozoic, Gondwanan, ice, age, GeoQUEST

Disciplines

Life Sciences | Physical Sciences and Mathematics | Social and Behavioral Sciences

Publication Details

Fielding, C. R., Bann, K. L., Maceachern, J. A., Tye, S. C. & Jones, B. G. (2006). Cyclicity in the nearshore marine to coastal, Lower Permian, Pebbley Beach Formation, southern Sydney Basin, Australia: a record of relative sea-level fluctuations at the close of the late Palaeozoic Gondwanan ice age. Sedimentology, 53 (2), 435-463.

CYCLICITY IN THE NEARSHORE MARINE TO COASTAL, LOWER PERMIAN, PEBBLEY BEACH FORMATION, SOUTHERN SYDNEY BASIN, AUSTRALIA: A RECORD OF RELATIVE SEA-LEVEL FLUCTUATIONS AT THE CLOSE OF THE LATE PALAEOZOIC GONDWANAN ICE AGE.

Christopher R. Fielding[1], Kerrie L. Bann[2], James A. MacEachern[3], Stuart C. Tye[4] & Brian G. Jones[5]

[1] – Department of Geosciences, 214 Bessey Hall, University of Nebraska-Lincoln, NE 68588-0340, USA

[2] – Ichnofacies Pty Ltd, 9 Sienna Hills Court SW, Calgary, Alberta, Canada T3H 2W3

[3] – Department of Earth Sciences, Simon Fraser University, Burnaby, British Columbia, Canada V5A 1S6 jmaceach@sfu.ca

[4] – Husky Energy, 707 8th Avenue SW, Calgary, Alberta, Canada

[5] – School of Earth and Environmental Sciences, University of Wollongong, NSW 2522, Australia

Corresponding Author: Christopher R. Fielding (cfielding2@unl.edu)

Running Title: sequence stratigraphy of Icehouse Permian strata, Australia

ABSTRACT

The Lower Permian (Artinskian to Sakmarian) Pebbley Beach Formation of the southernmost Sydney Basin in New South Wales, Australia, records sediment accumulation in shallow marine to coastal environments at the close of the Late Palaeozoic Gondwanan ice age. This paper presents a sequence stratigraphic re-evaluation of the upper half of the unit based on the integration of sedimentology and ichnology. Ten facies are recognized, separated into two facies associations. Facies Association A (7 facies) comprises variably bioturbated siltstones and sandstones with marine body fossils, interpreted to record sediment accumulation in open marine environments ranging from lower offshore to middle shoreface water depths. Evidence of deltaic influence is seen in several Association A facies. Facies Association B (3 facies) comprises mainly heterolithic, interlaminated and thinly interbedded sandstone and siltstone with some thicker intervals of dark grey, organic-rich mudstone, some units clearly filling incised channel forms. These facies are interpreted as the deposits of estuarine channels and basins. Throughout the upper half of the formation, erosion surfaces with several metres relief abruptly separate open marine facies of Association A (below) from estuarine facies of Association B (above). Vertical facies changes imply significant basinward shift of environment across these surfaces, and lowering of relative sea level on the order of 50 metres. These surfaces can be traced over several kilometres along depositional strike, and are defined as sequence boundaries. On this basis, at least nine sequences have been recognized in the upper half of the formation, each of which is <10 m thick, condensed, incomplete and top-truncated. Sequences contain little if any record of the lowstand systems tract, a more substantial transgressive systems tract and a highstand systems tract that is erosionally truncated (or in some cases, missing). This distinctive stacking pattern (which suggests a dominance of retrogradation and progradation over aggradation) and

the implied relative sea-level drop across sequence boundaries of tens of metres are remarkably similar to some other studies of continental margin successions formed under the Neogene icehouse climatic regime. Accordingly, it is suggested that the stratigraphic architecture of the Pebbley Beach Formation was a result of an Icehouse climate regime characterised by repeated, high-amplitude cycles of relative sea-level change.

Keywords Lower Permian, shallow marine facies, estuarine facies, sequence stratigraphy, icehouse.

INTRODUCTION

Much research has been devoted to documenting stratigraphic stacking patterns on continental margins, with particular reference to the stratigraphic consequences of cycles of sea-level change. To date, however, much of this research (e.g., Van Wagoner *et al*., 1990, 1991; Posamentier & Allen, 1999) has focused on successions formed under relatively benign climatic regimes (so-called “Greenhouse” periods of Earth history, such as the Mesozoic era). The architecture of continental margin sedimentary successions formed under “Icehouse” climatic regimes is, however, less well documented. The nature of stratal stacking patterns, including the character and scales of vertical facies cyclicity, are particularly poorly understood for successions of pre-Cenozoic age. Nonetheless, studies of more widely preserved Cenozoic successions, for which there are more precise and accurate geochronological constraints, should assist in the analysis of similar older successions. A variety of work has demonstrated that sea-level fluctuations during the Cenozoic Icehouse era were rapid, high frequency and of high

amplitude (10's to 100+ m: e.g., Zachos *et al*., 2001). Forcing mechanisms operating at orbital (Milankovitch) frequencies have been identified for several parts of the Cenozoic in a variety of areas worldwide (see reviews by Miller *et al*., 1991; Zachos *et al*., 2001). It is likely that these forcing mechanisms leave discernible imprints on the sedimentary record of continental margins.

The stratal architectures of nearshore marine successions deposited during the Cenozoic, particularly during the more severe Icehouse conditions of the Neogene, have been documented by a number of workers. For example, the Miocene Chesapeake Group of Maryland and adjacent regions of the eastern USA consists of a series of thin (typically a few m) cycles or "cyclothems" of predominantly shallow marine origin, bounded by regionally extensive erosion surfaces (Kidwell, 1984, 1989, 1997). In the Plio-Pleistocene Wanganui Basin succession in New Zealand, a large number of erosionally based cycles, up to a few 10's of metres in thickness, are attributed to deposition in nearshore marine environments under Milankovitch-band forcing frequencies (Naish & Kamp, 1997; Saul *et al*., 1999). A third example is given by the Oligocene to Miocene succession of the Victoria Land Basin, Antarctica, as investigated by the Cape Roberts Drilling Project. In a depositional setting proximal to the Antarctic continental margin, a series of 2-80 m (typically 10-25 m) thick erosionally based cycles have been recognized (Fielding *et al*., 2000, 2001a), recording repeated advances and retreats of glaciers during the period 34-17 Ma. Precise geochronological constraints have allowed the recognition of Milankovitch-band forcing on the section straddling the Oligocene-Miocene boundary (Naish *et al*., 2001).

The sequence architectures of these examples share much in common. All of the successions mentioned, as well as many more from the same time period, comprise stacks of relatively thin (< a few 10's of m), condensed, incomplete (in terms of systems tracts) and top-

truncated stratal cycles. It is conceivable that this stratigraphic architectural style is a characteristic of the Neogene Icehouse, or indeed of icehouse periods in general. In a review of the seismic stratigraphy of various continental margins, Bartek *et al*. (1991) proposed a cross-sectional stratal architecture that typifies the Neogene for continental margins that are comparable in terms of subsidence patterns. This architecture is one of several thin sequences, bounded by regionally extensive erosion surfaces (sequence boundaries) that stack in predominantly retrogradational to progradational (as opposed to aggradational) patterns, suggesting that accommodation space on continental margins was limited during this interval of time. Bartek *et al*. (1991) also show how this pattern contrasts with the more aggradational pattern of the underlying Paleogene succession. Thus, an increasing body of data suggests that the Neogene Icehouse climatic regime was responsible for a distinctive stratigraphic architecture on continental margins. In this paper, a similar stratigraphic stacking pattern is documented in the Early Permian of southeastern Australia, and the conclusion is drawn that it too arose from sediment accumulation during a period of repeated, large-scale cycles of relative sea-level change.

Two issues combine to limit understanding of pre-Cenozoic icehouse periods: 1. a general lack, to date, of robust geochronological frameworks; and 2. a lack of confidence in geological information originally used to diagnose glacial conditions in ancient rocks prior to the 1980's. These have led to enduring controversies over the timing, duration, character and even existence of pre-Cenozoic ice ages. The Late Palaeozoic Gondwanan Ice Age (LPGIA) is a case in point. In a widely cited authority on this period of the geological record, Veevers & Powell (1987) proposed that the acme of the ice age was brought about by a major orogenic event that created extensive upland areas across Gondwana in the mid-Carboniferous, that the event was

characterized in large part by the formation of a continental ice sheet of great areal extent, and that this ice age persisted from the mid-Carboniferous until the late Early Permian, some 55 m.y. The data upon which these assertions were based, at least in Australia, arose principally from regional geological investigations carried out in the 1960's. These data had not been tested rigorously against the more complete understanding of glacial depositional systems that were available by the 1980's, a problem indeed that has persisted to the present day.

More recently, efforts have been made to critically re-evaluate the stratigraphic record of the LPGIA in Australia (e.g., Dickens, 1996; Tye *et al*., 1996; Eyles *et al*., 1998; Eyles & Eyles, 2000; Isbell *et al*., 2003). An emerging theme, reviewed comprehensively by Isbell *et al*. (2003), is that rather than being a single, protracted glacial period within which glaciers waxed and waned, the LPGIA perhaps comprises three discrete glacial periods, each of a few m.y. duration, separated by non-glacial periods. Most recently, Jones & Fielding (2004) have proposed that the stratigraphic record in Queensland, NE Australia, preserves only three short periods of glaciation, each 1-4 m.y. This and other hypotheses regarding the timing and duration of glaciation have as yet to be rigorously tested by correlation to other regions.

Most of the successions that record Late Palaeozoic glacial events in the Queensland record occur in continental basins. Elsewhere, in eastern Queensland and New South Wales, however, coastal to nearshore marine successions were accumulating in the coeval Bowen-Gunnedah-Sydney Basin system, during the Early Permian, within a north-south elongate seaway that formed initially as a failed rift (Fielding *et al*., 2001b). One such unit is the Pebbley Beach Formation (PBF) of the southern Sydney Basin in New South Wales, the subject of the present paper. As far as can be determined from mainly biostratigraphic constraints (e.g., Briggs, 1998), the PBF records one of the glacial intervals mentioned above, of late Sakmarian to early

Artinskian age. The PBF is interpreted to preserve a shallow marine record of the glacial interval in its lower half, and the immediate postglacial period in its upper half. In this paper, an analysis of stratal stacking patterns within the upper half of the PBF is presented, with a revised sequence stratigraphic framework for the unit. It is suggested that the distinctive stacking patterns observed may be a consequence of large-scale and high-frequency relative sea-level fluctuations such as are characteristic of Icehouse climatic regimes.

GEOLOGICAL SETTING AND PREVIOUS WORK

The Pebbley Beach Formation crops out in a series of spectacular coastal headlands and cliffs in southern New South Wales, Australia (Fig. 1). The unit forms part of the Permian succession of the southern Sydney Basin, contiguous with the Gunnedah and Bowen Basins in northern New South Wales and Queensland, respectively (Fig. 2). The unit, of Sakmarian to Artinskian age, forms the easternmost tract of an eastward-thinning, coarse clastic wedge (Figs 2, 3). In proximal areas to the west, the unit comprises stacked alluvial conglomerates and sandstones of the Yadboro Conglomerates, which pass eastward (down-depositional dip) into, and are overlain by, a more lithologically variable unit termed the Yarrunga Coal Measures. The PBF forms an eastward extension of the Yadboro Conglomerate and possibly in part the Yarrunga Coal Measures, and is interpreted as a distal equivalent to those facies (Figs 2, 3). These formations are part of a suite of similar coarse clastic wedges recording sediment dispersal eastward along the western margin of a developing, north-south-elongate seaway (or possibly open continental margin) during Sakmarian to Artinskian times (Fig. 3). These units characteristically exhibit abrupt lateral facies and thickness variations, and locally host thick (<40 m), areally restricted

coal bodies (such as in the Greta Coal Measures of New South Wales and the Blair Athol Coal Measures of Queensland). For these reasons, coupled with their lateral confinement within older, extensional depocentres, they were regarded by Fielding *et al*. (2001b) as having formed late during a phase of modest crustal extension (Figs. 2, 3). The subsidence regime is interpreted to have been temporally and spatially irregular, with some intervals of rapid, perhaps coseismic subsidence in certain areas. Widespread marine transgressions established shallow marine conditions across the entire basin system during the late Sakmarian stage (at about the Tastubian/Sterlitamakian boundary), linking the previously discrete extensional basins into a single connected basin that was probably contiguous with the palaeo-Pacific Ocean to the east (Fig. 3).

The PBF is widely regarded to have formed in coastal and nearshore marine environments (Gostin & Herbert, 1973; Tye *et al*., 1996; Tye, 1995; Bann, 1998; Bann *et al*., 2004). An analysis by Eyles *et al*. (1998), however, interpreted the unit to be the product of entirely marine depositional environments, occupying inner to outer shelf water depths. Eyles *et al*. (1998) also presented a sequence stratigraphic analysis of the PBF, in which they inferred a series of relative sea-level fluctuations and attributed these to a combination of tectonic, sediment supply and glacio-eustatic sea level drivers in a glacially-influenced marine setting.

The present work has established that the lower and upper halves of the PBF preserve quite different facies assemblages, and are interpreted to record distinct palaeoenvironmental conditions. The lower half of the formation contains a repetitive series of 1-5 m thick cycles each comprising, in ascending order, laminated, unbioturbated siltstone, capped by a hiatal surface with subtending unlined, coarse-grained burrow fills, and overlain by crudely stratified diamictite. These are interpreted to record glacial-interglacial cycles in a shallow glacimarine

environment. This succession grades upward through more homogeneous, bioturbated sandstones, into the upper association that is the subject of the present paper.

The upper half of the PBF preserves a number of prominent erosion surfaces, some of which form channels. While earlier workers interpreted these features and their mainly heterolithic fills as coastal, estuarine channels (Gostin & Herbert, 1973; Mifsud, 1990; Tye, 1995; Tye *et al*., 1996; Bann, 1998), Eyles *et al*. (1998) regarded them as having formed in open marine settings by unspecified erosional processes. Eyles *et al.*'s (1998) figure 7 shows many of the erosion surfaces as recording abrupt deepening of the depositional surface, i.e., as transgressive surfaces of erosion, although they also argue for shallowing in certain cases (p. 149-150). Eyles *et al*. (1998) noted that previous workers have interpreted these features as estuarine channel fills, but they appear not to favour this interpretation. Furthermore, their classification of the heterolithic facies that overlie the erosion surfaces as mid-outer shelf deposits ("Facies Association 5": see their figures 7 and 10) seems to be at odds with their assertion that the channels formed in "relatively shallow water" (p. 149 and 150).

In this paper, the erosion surfaces in the PBF are shown to be overlain by estuarine facies, rather than by deposits of mid-outer shelf environments (see also Bann *et al*., 2004). These predominantly heterolithic sandstone-siltstone strata in many cases abruptly overlie offshore marine facies that superficially are lithologically similar, making recognition of the contact challenging. The pronounced dislocation in facies across these surfaces indicates that they record 10's of m of erosional incision and relative sea level fall. This, together with the lateral continuity of the surfaces over at least several kilometres, suggests strongly that the erosion surfaces delimit sequence boundaries. The <10 m thick sequences between these boundaries

record repeated, high-amplitude relative sea-level fluctuations at a time that is likely to have experienced major fluctuations in ice storage in palaeo-polar Gondwana.

FACIES ANALYSIS

A facies and sequence stratigraphic analysis of the upper half of the PBF, emphasizing the role of ichnological data, was presented by Bann *et al*. (2004). This combined lithofacies/ichnofacies scheme is extended and further details of the sedimentology are given here. The facies scheme comprises two facies associations. Facies Association A contains seven facies (A1-A7) and records sediment accumulation in open, nearshore marine environments, some of which show deltaic influences (cf. Bann & Fielding, 2004; MacEachern *et al*., 2005) (Table 1). Facies Association B consists of three facies (B1-B3), and records deposition in estuarine channels and basins (Table 1). Following a brief review of Facies Association A, the principal focus is on the facies characteristics of Association B, including external and internal bounding surfaces, sediment body geometry, physical and biogenic sedimentary structures, palaeocurrent relationships and contacts with enclosing facies.

Facies Association A

Description

Facies Association A comprises seven facies, A1-A7 (Table 1, Figs 4-7), that range from fine-grained to progressively coarser-grained upward. Concomitant with this change in grain-size the facies also grade from most pervasively bioturbated to least pervasively bioturbated (see Bann *et*

al., 2004, for further details). All facies, but particularly the fine-grained variants, contain sparse to abundant, dispersed, outsized clasts of basement lithologies (principally quartzite, phyllite, chert, vein quartz, granite and volcanic rocks).

Facies A1 consists of thoroughly bioturbated, muddy siltstone with few if any preserved primary sedimentary structures (Fig. 4). Glendonites, carbonate pseudomorphs that are thought to be after the calcium carbonate hexahydrate mineral ikaite, are common locally in this facies. Rare dispersed gravel and hummocky cross-stratified (HCS) sandstone lenses are the principal physical features (Fig. 4B, C), while the trace fossil suite contains a diverse mixture of deposit-feeding and grazing structures representing a distal expression of the *Cruziana* Ichnofacies (Fig. 4C).

Facies A2 comprises thoroughly bioturbated sandy siltstone, with an increased incidence of discrete, thin HCS sandstone beds. The trace fossil suite contains a diverse mixture of complex deposit-feeding, detritus-feeding, grazing and foraging structures with less common vertical structures, and corresponds to the archetypal *Cruziana* Ichnofacies. Vertical burrows represent elements of the *Skolithos* Ichnofacies and indicate opportunistic colonization of the thin HCS beds by suspension-feeding infauna.

Facies A3 contains interbedded bioturbated sandy siltstone and laminated sandstone, showing variable levels of bioturbation (Fig. 5). Sandstone beds preserve HCS with associated oscillation and combined-flow ripples. The trace fossil suite is diverse, recording a wide variety of feeding strategies, consistent with the archetypal *Cruziana* Ichnofacies (Fig. 5C). Vertical structures are common and indicate opportunistic colonization by elements of the *Skolithos* Ichnofacies (Fig. 5C). Facies A4 comprises thoroughly bioturbated muddy sandstone with physical structures comparable to Facies A3, and a trace fossil suite characterized by robust

deposit- and detritus-feeding structures, vertical domiciles, and grazing and foraging structures (Fig. 6). This diverse assemblage represents a proximal expression of the *Cruziana* Ichnofacies .

Facies A5 consists of interbedded laminated sandstone, bioturbated muddy sandstone, and dark claystone. The facies contains well-preserved, large-scale HCS, and distinctive beds of coarse-grained sandstone to granule conglomerate preserved as large, symmetrical (oscillation) ripple forms (cf. Forbes & Boyd, 1987; Cheel & Leckie, 1992, Fig. 6). The trace fossil suite contains a diverse mixture of robust detritus-, deposit- and suspension-feeding structures, grazers and foragers, and escape traces. It represents a diverse, proximal expression of the *Cruziana* Ichnofacies (Fig. 6). The dark claystone interbeds are generally not burrowed and contain common synaeresis (subaqueous shrinkage) cracks, as well as an abundance of phytodetrital material (Fig. 6B-E).

Facies A6 (not included in Bann *et al*., 2004) comprises amalgamated, tabular beds of sparsely bioturbated sandstone that display large-scale HCS and unidirectional cross-bedding. The trace fossil suite comprises ichnogenera reflecting sedentary deposit-feeding and suspension-feeding behaviours, and represents a distal expression of the *Skolithos* Ichnofacies. Facies A7 consists of bioturbated, poorly sorted, laterally variable sandstones, with a wide variety of sedimentary structures including unidirectional cross-bedding and symmetrical wave ripples (Fig. 7). Bioturbation intensities and assemblage diversities are also variable throughout the facies. Sedentary and mobile deposit-feeding, opportunistic grazing, and suspension-feeding behaviours dominate the ichnological suite (Fig. 7C). The trace fossil suite represents a distal expression of the *Skolithos* Ichnofacies. The upper surface of one unit within Facies A7, which is well-exposed at Mill Point and Clear Point, is covered with articulated *Eurydesma hobartense* shells.

Interpretation

There is substantial evidence to suggest that the facies of Association A were deposited in an open marine setting. This interpretation is supported by the abundance of marine invertebrate fossils and the ichnological signatures, which reflect deposition in well oxygenated offshore to shoreface environments that experienced intermittent, high-energy storms. A range of depositional environments from lower offshore (A1), upper offshore (A2) and offshore transition (A3), to distal lower shoreface (A4), proximal lower shoreface (A5) and middle shoreface (A6) are indicated (see Bann *et al*., 2004, for more details). Facies A7 contains evidence of sediment accumulation in a range of potential water depths, but its vertical context indicates that it formed during periods of transgression and the facies is, therefore, interpreted as a transgressive sand sheet deposit. Several of the facies contain physical structures and ichnological signatures that suggest deposition within proximity to contemporaneous deltas. In particular, the unbioturbated, carbonaceous mudstone partings with associated synaeresis cracks are consistent with fresher water discharge events with associated phytodetrital pulses, such as are typical of some delta front and prodelta settings (Raychaudhuri and Pemberton, 1992, Saunders *et al*., 1994, Coates & MacEachern, 1999; Bann & Fielding, 2004, MacEachern *et al*., 2005). Limited direct evidence of delta front deposition was identified in the PBF, however, and sediment accumulation is interpreted to have occurred in shallow marine environments alongshore from a delta (either downdrift of distributaries or possibly updrift of the active lobes). The abundance of dispersed clasts in Association A facies, their variable long-axis orientations with respect to bedding, and the fact that they puncture the lamination of immediately underlying strata, indicate that some

sediment was dropped or dumped from floating ice The presence of glendonites indicates that the sea-floor environment must have been cold and at times dysaerobic (Carr *et al*., 1989).

Facies Association B

Description

Association B comprises three fine-grained or heterolithic sandstone-siltstone facies that for the most part lack dispersed coarse clasts (Figs 8-10). All three facies occur together in units <9 m thick that overlie erosion surfaces. Association B facies commonly pass laterally into one another, a feature that is not evident in the facies of Association A. Erosion surfaces have relief of <6 m in coastal exposures, particularly at the southern end of Point Upright (Figs 1, 8A, 10A), and cut through a variety of lithologies, including sandstone-dominated middle and lower shoreface deposits of Association A. Surfaces are locally mantled by single clast-thick pebble lags (Fig. 10B), and concentrations of flattened, coaly plant compressions and petrifactions of fossil trees are also common. In some cases, the intervals immediately underlying the surfaces are strongly disrupted by soft-sediment deformation, particularly load casts and convolute bedding, which may be truncated by the erosion surface itself. Many such erosion surfaces, however, separate heterolithic facies of Association A below from heterolithic facies of Association B above (e.g., Fig. 9A, 11), making the recognition of some surfaces a challenging task. In such cases, the principal diagnostic criteria are the variety and intensity of bioturbation and degree of preservation of physical sedimentary structure (Fig. 11).

Association B facies are sparsely to moderately bioturbated (Table 1, Figs 8-10). The ichnological signatures are characterised by low diversity assemblages containing simple

deposit-feeding and vertical dwelling (suspension-feeding?) structures that reflect the activities of resilient trophic generalists. Fugichnia (escape or equilibrium adjustment structures) are also common in some intervals. The assemblage is restricted (impoverished), comprising elements of both the *Skolithos* and *Cruziana* Ichnofacies, here termed a mixed *Skolithos-Cruziana* Ichnofacies, and contrasts markedly with the diverse, archetypal *Cruziana* Ichnofacies that characterises the otherwise lithologically similar offshore marine deposits of Facies A1 and A2 (cf. Bann *et al*., 2004).

Facies B1 comprises sparsely bioturbated, interbedded and interlaminated, fine-grained sandstone and siltstone, with a discrete depositional dip that defines inclined heterolithic stratification (IHS, *sensu* Thomas *et al*., 1987) and, in many cases, a channelised form in cross-section (Figs. 8A, 12, 13). Individual channels are <6 m deep and typically 100-250 m wide, where dimensions can be determined. At the margins of channel forms, Facies B1 passes laterally into thin units of Facies B2. IHS sets range up to 6 m thick, with apparent dips reaching maximums of 25^0, flattening tangentially at the set base (Fig. 8A, 12). While many Facies B1 bodies comprise a single set of IHS, a few (notably an interval exposed at Mill Point and on the south side of Clear Point), are composite units comprising up to at least four storeys (Fig. 13). Individual storeys are traceable over several hundred metres along the cliff line at Mill Point by physical correlation (Fig. 13), but the equivalence of these storeys with similar units on Clear Point is more speculative.

Internally, IHS sets comprise thinly-bedded sandstone/siltstone alternations (sandstone beds <5 cm, sand:silt ratios typically around 50:50: Fig. 8B, C) that preserve a variety of current ripple-scale interlamination structures, with thicker sandstone beds at intervals. In some cases, notably at the south end of Point Upright, the thicker sandstone beds show apparent intraset

bedding, with internal bedding surfaces that either are inclined very gently up the dip of the large-scale IHS or are flat-lying (Fig. 8A). Interlamination structures comprise a full spectrum from pinstripe (linsen), through lenticular and wavy bedding, to flaser lamination in the more sand-dominated intervals (Fig. 8C). In all cases, the internal cross-lamination is largely undisturbed by bioturbation (Fig. 8C), although locally it may be disrupted by soft-sediment deformation in the form of convolute bedding or overturned slump folding. Cross-lamination structures are predominantly unidirectional, (i.e., current-generated); although foreset dip directions typically describe bimodal (commonly bipolar) distributions (Fig. 8C). The modal azimuths of small-scale structures typically lie at high angles (60-120^{o}) to the azimuth of dip of the large-scale, IHS sets (e.g., Figs 12, 13). Some ripple sets show evidence of wave modification, such as reversed asymmetry of the external ripple form relative to the internal cross-lamination, bidirectional cross-lamination within a single set, or symmetrical drape over a unidirectional cross-lamination set (Fig. 8C). Synaeresis cracks are abundant in this facies. Trace fossils are low in abundance and assemblage diversity is extremely impoverished. The suite contains only the simple feeding and dwelling structures of trophic generalists and corresponds to a highly stressed expression of the mixed *Skolithos*-*Cruziana* Ichnofacies (Bann *et al*., 2004).

The basal portion of some Facies B1 bodies comprises trough cross-bedded, coarse- to very coarse-grained or even pebbly sandstone (Facies B1a: Fig. 13). In such cases, the basal erosion surface commonly shows load casts of the coarse-grained facies projecting downward into the underlying sediment. The trough cross-sets are typically 0.3-0.6 m thick, with a few up to 1.0 m. Their foreset dip directions typically describe bimodal to bipolar distributions (Fig. 13). Flattened, coalified plant compressions are also commonly preserved within the coarse-grained

sandstones. These coarse-grained sandstones typically pass upward abruptly into the heterolithic lithologies described above (Fig. 13).

Facies B2 comprises heterolithic, interlaminated and thinly interbedded fine-grained sandstone and siltstone, similar to the lithology of Facies B1 but with the important distinction that bedding is flat and tabular in all orientations, concordant with the lower and upper bounding surfaces (Fig. 9). A similar range of small-scale interlamination structures is present, with an increased incidence of wave-modified current ripple cross-lamination relative to Facies B1. Furthermore, small-scale hummocky cross-stratification (sets with bedform amplitude of 0.03-0.1 m, wavelength 0.15-0.4 m) is locally well-developed, and symmetrical wave ripples are abundantly developed on some bedding planes. An additional, highly distinctive sedimentary structure, seemingly restricted to this facies, is a rhythmic alternation of fine-grained sandstone and siltstone (individual laminae 1-3 mm thick), either in flat lamination or within sets of current ripple cross-lamination (Fig. 9B, D). Synaeresis cracks and other soft-sediment deformation structures are well-developed, particularly in the uppermost part of certain intervals below overlying Association A facies. Detrital plant debris is less abundant, and petrified log casts are absent, as are basal clast layers. Facies B2 contains a sporadically distributed, moderately diverse trace fossil assemblage (Fig. 9C). Trace fossil abundances and diversities change markedly both vertically and laterally within the facies, suggesting spatial and temporal variations in the degree of marine influence (Fig. 9C). Bioturbation intensities are highly variable. The trace fossil suite contains a mixture of simple deposit- and less common suspension-feeding structures, and corresponds to a stressed expression of the *Cruziana* Ichnofacies. The sporadically distributed, more marine influenced intervals tend to be characterized by the mixed *Skolithos*-*Cruziana* Ichnofacies (Bann *et al*., 2004).

Facies B3 consists of medium to dark grey to black, laminated to blocky, fine-grained siltstone and claystone, with uncommon interlaminated fine-grained sandstone (Fig. 10A-C). Some occurrences show flat internal bedding with a tabular external geometry, while others fill channel forms as described above (Fig. 10A). A sulphurous smell is evident, and discrete small pyrite crystals are visible locally. Apart from linsen and lenticular bedding in the rare, thin sandstone laminae, the only physical sedimentary structure evident is common normal grading over 1-5 mm intervals. Small rounded dispersed gravel-sized clasts were noted in some exposures (Fig. 10B). This facies is characterised by having virtually no evidence of bioturbation, other than burrows that subtend from overlying units (Fig. 10C, Bann *et al.*, 2004).

Interpretation

Facies Association B comprises an array of heterolithic and fine-grained terrigenous clastic deposits, characterised by generally low-energy, current-generated, wave-modified and, to a lesser extent, wave-generated sedimentary structures, with abundant plant fossils, a lack of marine invertebrate body fossils, and a low diversity, low abundance *Cruziana* Ichnofacies. This, together with the evidence for reversing flows (bimodal to bipolar palaeocurrent distributions) is suggestive of coastal environments in which the principal depositional mechanism is from tides, and where waves play a subordinate role and fluvial outflow is minimal (cf. Boyd *et al.*, 1992). The basal, trough cross-bedded grits of Facies B1a are suggestive of more substantial fluvial sediment supply at certain times, following excavation of the major erosion surfaces on which these facies lie.

Broadly estuarine environments of deposition are envisaged for Facies Association B (Bann *et al.*, 2004). Facies B1 is interpreted to record sediment accumulation in sinuous

estuarine channels of moderate size (<6 m x 250 m, at least). Channel forms are evident from the geometry of the basal erosion surface, while lateral accretion patterns are evident from the relationship of IHS dip directions to the migration directions of small-scale structures (Figs 12, 13). Facies B2 represents sediments deposited in laterally adjacent estuarine basins (largely shallow subtidal, since little if any evidence of emergence was noted). Facies B3 records passive fill of both channels and basins. Association B facies in all cases abruptly overlie erosion surfaces that cut into a variety of Association A facies, and form discrete intervals (a few metres in thickness) that can be traced laterally over several kilometres.

Overall Depositional Setting

The facies recognized in the upper half of the PBF suggest a coastal to shallow water, open marine environment of deposition. Sedimentary structures in Association A facies indicate a wave- and storm-dominated shoreface to offshore setting with deltaic influence. The ubiquitous presence of outsized clasts of basement lithologies indicates ice-rafting of material to the marine environment, possibly from seasonal river and sea ice sources (Bann, 1998). Furthermore, the abundance of the thick-shelled bivalve *Eurydesma* (Dickins, 1978; Runnegar, 1979) and of glendonites (Carr *et al*., 1989) are widely regarded as evidence of cold sea floor conditions at this time (<6° C: Bischoff *et al.*, 1993). Given this and the evidence of glaciation in Australia immediately prior to this time, the PBF can be regarded as the product of coastal to shallow marine deposition in a high-latitude setting, perhaps analogous to the modern coast of northeastern Canada or Patagonia. The abundance of fine-grained estuarine facies in the upper PBF, however, suggests coastal estuaries that were dominated by low-energy current deposition.

In the spectrum of known estuarine depositional settings (Dalrymple *et al*., 1992), a series of funnel-shaped estuaries with barred entrances (consistent with the evidence for storm-driven processes in the over- and underlying marine facies) seems appropriate for the upper PBF. In this setting, sinuous channels migrated across and into shallow but permanent brackish-water basins, delivering sediment to the coastal zone. Comparable facies assemblages and interpretations have recently been documented by Shanmugam *et al*. (2000), Takano & Waseda (2003) and Holz (2003).

STRATIGRAPHIC STACKING PATTERNS

Graphic logs of the three key sections (Clear Point, Mill Point and Point Upright, from north to south) show an apparent complex interbedding of the various lithofacies, with little obvious vertical cyclicity evident from grain-size variations (Figs 14-16). However, through the identification and correlation of the various erosion surfaces, a coherent high-resolution stratigraphic framework can be constructed (Figs 17, 18). Our correlations have established that the erosion surfaces noted in the cliff exposures are laterally extensive, being traceable (physically across substantial portions of the coastal section) over several kilometers (Fig. 17), and can therefore be considered “key surfaces”. The surfaces separate facies recording generally offshore marine to lower shoreface environments (Facies Association A) below, from estuarine facies (Facies Association B) above, a substantial, abrupt dislocation in terms of formative water depth. The abrupt shallowing across these surfaces can be estimated conservatively at 50 m, based on published estimates of water depths to storm wave base in storm-dominated, open marine environments (see, for example, reviews in Brenchley, 1989; Walker & Plint, 1992) and

the fact that no evidence for subaerial exposure is preserved in these rocks. These surfaces therefore satisfy many of the criteria for sequence boundaries, namely: they are laterally extensive surfaces, record abrupt truncation of underlying facies, and show an abrupt upward shallowing in formative water depth (basinward shift of facies). Accordingly, we interpret the erosion surfaces overlain by estuarine facies as sequence boundaries, and subdivide the upper PBF into a succession of nine discrete sequences (Figs 17, 18), ranging in thickness from <1 m to 10 m.

The vertical facies succession in a typical upper PBF sequence is as follows: estuarine channel or basin (Facies B1-B3), abruptly overlain by offshore transition to offshore facies (Facies A1-A3), that locally coarsens-upward into lower shoreface (Facies A4-A5) deposits before truncation by the next erosion event. Individual sequences vary with respect to the vertical facies succession along the coastal section from north to south, but only in the extent to which the uppermost shoreface facies are preserved; that is, facies architecture among Association A facies are tabular and sheet-like in a depositional strike orientation. Given this and the characteristics of the erosion surfaces established above, the vertical facies pattern can be interpreted genetically, as follows: 1. the erosion surfaces are sequence boundaries, recording tens of metres of sea level fall along with incision into the previous sequence (typically highstand systems tract deposits); 2. the coarse-grained, trough cross-bedded sandstones (Facies B1a), where present, record late lowstand systems tract deposition in fluvial to estuarine environments; 3. the heterolithic estuarine deposits (Facies B1-B3) record backfilling of estuaries during early phases of sea-level rise (late lowstand to early transgressive systems tract); 4. the abrupt upward transition into offshore marine deposits (Facies A1-A2) records rapid flooding during the main phase of sea-level rise, with the maximum flooding surface recorded in the

finest-grained offshore deposits; 5. the overlying coarsening-upward succession into lower shoreface sandstones (Facies A3-A5) records progradation during the succeeding highstand systems tract, before; 6. ensuing sea-level fall resulted in erosion of much of the highstand systems tract, forming a new sequence boundary. Where transgressive systems tract facies directly overlie an erosion surface, the resulting discontinuity can be considered a coincident sequence boundary/ flooding surface (FS/SB) (Bann *et a*l., 2004). Nine sequences are defined within the upper half of the PBF. Of these, two (Sequences 1 and 7 on Fig. 18) are not readily divisible into systems tracts but rather display stacked coarsening-upward parasequences. The remainder, however, display the architecture summarized above. Indeed, Sequences 4 and 5 are preserved over much of the outcrop only as estuarine facies, are highly amalgamated, and may conceal additional sequences (Fig. 13).

Little can be said concerning the rate of sea-level fall from the preserved facies patterns, but the rate of sea-level rise must have been rapid to produce the observed facies transitions over such short vertical intervals. It is also likely that highstands were relatively short-lived, since few well-established highstand deposits are preserved within the upper PBF. The general lack of coarse-grained highstand facies in the succession (which contrasts with the sandstone-dominated formations that underlie and overlie the PBF) also suggests that either they were never deposited in this area or substantial volumes of sand were removed by erosion during periods of falling sea-level and exported offshore.

The issue of sequence boundary cross-sectional geometry within the upper PBF is also relevant, since the possibility arises that they could record the seaward portions of incised valleys excavated during falls and lowstands of sea-level. Figure 17 shows the correlation of logged sections over the extent of coastal outcrop. It has been simplified to emphasise the cross-

sectional form of the sequence boundaries and overlying and other key surfaces. The surfaces clearly show erosional relief of up to several metres, possibly in addition to the tens of metres of incision inferred from vertical facies dislocations across the sequence boundaries. Furthermore, individual channels are in places (particularly at Point Upright, in the far south of the outcrop belt) inset relatively steeply, by as much as 6 m into the bases of these more gently sloping sequence boundaries. The fact that these estuarine systems and their facies are preserved at all, particularly within a transgressive systems tract, suggests that they must, by definition, occupy discrete, shore-perpendicular (or more oblique) topographic lows. The sequence boundaries also conform to most definitions of incised valleys (given the context of a downdip, coastal setting): 1. they are significant topographic features with considerable relief and kilometres of lateral extent in the depositional strike orientation; 2. they are at a scale significantly larger than that of channels that occupy their bases; 3. they show a pronounced basinward shift of facies; and 4. internal facies architectures display predominantly onlap relationships with the valley margins (cf. Dalrymple *et al*., 1992, 1994; Schumm & Ethridge, 1994; Zaitlin *et al*., 1994). On this basis, we tentatively ascribe the upper PBF estuarine systems to deposition in the downdip portions of incised valleys of indeterminate width. An alternative explanation, that these sequences overlie surfaces exhumed without any valley incision, is considered less likely but nonetheless cannot be discounted.

DISCUSSION

The overall vertical facies architecture of the upper PBF sequences is quite unlike the generic continental margin sequence composition predicted by standard models (e.g., Van Wagoner *et*

al., 1990; Posamentier & Allen, 1999), but is much more closely comparable to examples taken from some Neogene successions (Kidwell, 1989; Naish & Kamp, 1997, Fielding *et al*., 2000, 2001b) that were formed under a severe Icehouse regime (e.g., Zachos *et al*., 2001). PBF sequences are dominated by the transgressive systems tract, and show only local preservation of the lowstand systems tract and the highstand systems tract. Furthermore, PBF sequences are thin (<10 m), condensed, incomplete (in terms of systems tracts) and strongly top-truncated, as are the Neogene examples cited above. Accumulation of the upper PBF occurred shortly after a known glacial period (Isbell *et al*., 2003; Jones & Fielding, 2004), and within a longer interval of icehouse conditions during which variations in polar ice volumes are likely to have driven large-scale sea-level cyclicity.

The repetition of abrupt upward shallowing trends of approximately the same magnitude in the PBF argues against both an underlying tectonic control and an isostatic (direct loading or forebulge formation) driver for the cyclicity. Accordingly, we suggest that the observed patterns are most readily explained as glacio-eustatic cycles of sea-level change. Certainly, the vertical facies patterns are consistent with what is known about magnitudes and rates of change of sea-level rise and fall during Pleistocene glacial cycles, with rapid rises and short highstands being the norm (e.g., Lambeck & Chappell, 2001).

The low rates of accumulation during sea-level rise and highstand recorded in the upper PBF are also similar to many modern (post- or ?inter-glacial) coastal settings, such as the northeast coast of Australia (e.g., Larcombe & Carter, 1998, 2004) and the eastern seaboard of the USA (e.g., McHugh *et al*., 2004). The study of the Hudson River estuary and shelf is possibly a detailed analogue to the situation envisaged for the upper PBF. There, Holocene sediment accumulation is restricted to a wedge-shaped body in dip-parallel cross-section that

downlaps onto the underlying sequence boundary downdip on the inner shelf and is truncated by a nascent sequence boundary updip in the upstream portion of the estuary (McHugh *et al*., 2004).

The depositional cycles characterizing the Neogene examples cited above accumulated under the control of Milankovitch-band orbital frequencies, operating either singly or in some combination. Such controls seem to be prominent during intervals of icehouse climate, and thus a Milankovitch signal might be expected in the upper PBF. Best estimates from biostratigraphic data and lithostratigraphic correlations suggest that the PBF records c. 10 m.y. of Early Permian time. The upper half of the formation contains at least nine sequences, suggesting perhaps operation of 400 ka cycles. However, the lower half of the formation contains quite a different facies assemblage from the upper half, and may have accumulated at substantially different rates. Whatever the timeframe and controlling mechanism(s) under which the upper PBF sequences formed, stratigraphic patterns indicate that this forcing mechanism operated consistently throughout accumulation of the section. The magnitudes of sea-level fall implied by the PBF sequences (of the order of 50 m) are consistent with the more conservative estimates of contemporaneous sea-level fall based on studies of northern hemisphere “cyclothems” (60-70 m), but not with some of the larger estimates from that region (100-200 m: see discussion in Isbell *et al*., 2003).

CONCLUSIONS

The upper Pebbley Beach Formation in the southern Sydney Basin of New South Wales, Australia, comprises an array of depositional facies that record a variety of nearshore open marine and low-energy estuarine environments. Several of the open, shallow marine facies show

evidence of a deltaic influence, perhaps indicating that the study area occupied a position downdip or along strike from a delta. Estuarine facies at several stratigraphic levels overlie pronounced, laterally extensive erosion surfaces interpreted as sequence boundaries. Facies dislocation across these surfaces suggests sea-level falls of c. 50 m with some erosion of shallow marine strata, suggesting that the formation preserves a record of high-amplitude relative sea-level fluctuations. This, together with the cross-sectional geometry of the sequence boundaries, suggests that they may represent the downdip manifestation of incised valleys formed in lowland continental settings during relative sea-level falls. The <10 m thick sequences preserved between sequence boundaries are thin, condensed, incomplete (in terms of systems tracts) and top-truncated. This architecture is somewhat different from that predicted by published sequence stratigraphic models, but is similar in many respects to continental margin successions formed during the Neogene Icehouse climate regime. Given this and the proximity between timing of Pebbley Beach Formation accumulation and a known period of glaciation elsewhere in eastern Australia, we attribute this architectural style to accumulation under conditions of rapid, high-frequency and high-magnitude sea-level fluctuations that may have been glacio-eustatic.

ACKNOWLEDGEMENTS

This research was funded in part by the Mr & Mrs JB Coffman Endowment in Sedimentary Geology at the University of Nebraska-Lincoln, and latterly by NSF grant EAR-0417578 to C.R. Fielding and T.D. Frank. J.A. MacEachern received funding for fieldwork from a Canadian Natural Sciences and Engineering Research Council Discovery Grant no. 184293. Tracy Frank and Fiona MacEachern participated in the fieldwork and offered valuable insights. Reviews of

the submitted manuscripts by John Isbell, Carolyn Eyles, and Sedimentology Editor Peter Haughton led to significant improvement of the paper.

REFERENCES

Bann, K.L. (1998) *Ichnology and Sequence Stratigraphy of the Early Permian Pebbley Beach Formation and Snapper Point Formation in the Southern Sydney Basin*. PhD Thesis, University of Wollongong (unpubl.).

Bann, K.L. and Fielding, C.R. (2004) An integrated ichnological and sedimentological comparison of non-deltaic shoreface and subaqueous delta deposits in Permian reservoir units of Australia. In: *The Application of Ichnology to Palaeoenvironmental and Stratigraphic Analysis* (Ed. D. McIlroy), *Geol. Soc. London Spec. Publ*., **228**, 273-310.

Bann, K.L., Fielding, C.R., MacEachern, J.A. and Tye, S.C. (2004) Differentiation of estuarine and offshore marine deposits using integrated ichnology and sedimentology: Permian Pebbley Beach Formation, Sydney Basin, Australia. In: *The Application of Ichnology to Palaeoenvironmental and Stratigraphic Analysis* (Ed. D. McIlroy), *Geol. Soc. London Spec. Publ*., **228**, 179-211.

Bartek, L.R., Vail, P.R., Anderson, J.B., Emmet, P.A. and Wu, S. (1991) Effect of Cenozoic ice sheet fluctuations in Antarctica on the stratigraphic signature of the Neogene. *J. Geophys. Res*., **96**, 6753-6778.

Bischoff, J.L., Fitzpatrick, J.A. and Rosenbauer, R.J. (1993) The solubility and stabilization of ikaite ($CaCO_3.6H_2O$) from 0° to 25° C: environmental and paleoclimatic implications for thinolite tufa. *J. Geol*., **101**, 21-33.

Boyd, R., Dalrymple, R.W. and Zaitlin, B.A. (1992) Classification of clastic coastal depositional environments. *Sed. Geol.*, **80**, 139-150.

Brenchley, P.J. (1989) Storm influenced sandstone beds. *Modern Geol*., **9**, 369-396.

Briggs, D.J.C. (1998) *Permian Productidina and Strophalosiidina from the Sydney-Bowen Basin and New England Orogen: systematics and biostratigraphic significance*. Association of Australasian Palaeontologists, Memoir, **19**, 258pp.

Carr, P.F., Jones, B.G. and Middleton, R.G. (1989) Precursor and formation of glendonites in the Sydney Basin. *Austr. Mineral.*, **4**, 3-13.

Coates, L., and MacEachern, J.A. (1999) The ichnological signature of wave- and river-dominated deltas: Dunvegan and Basal Belly River formations, West-Central Alberta. In: *Digging Deeper, Finding a Better Bottom Line* (Eds. B. Wrathall, G. Johnston, A. Arts, L. Rozsw, J.-P. Zonneveld, D. Arcuri, and S. McLellan). *Canadian Society of Petroleum Geologists & Petroleum Society, Core Conference*, 99-114.

Cheel, R.J. and Leckie, D.A. (1992) Coarse-grained storm beds of the Upper Cretaceous Chungo Member (Wapiabi Formation), southern Alberta, Canada. *J. Sed. Petrol*., **62**, 933-945.

Dalrymple, R.W., Zaitlin, B.A. and Boyd, R. (1992) Estuarine facies models: conceptual basis and stratigraphic implications. *J. Sed. Petrol*., **62**, 1130-1146.

Dalrymple, R.W., Boyd, R. and Zaitlin, B.A. (1994) History of research, valley types, and internal organization of incised-valley systems: Introduction to the volume. In: *Incised Valley Systems: Origin and Sedimentary Sequences* (Eds. R. Boyd, B. Dalrymple and B. Zaitlin), *SEPM Spec. Publ*., **51**, 3-10.

Dickins, J.M. (1978) Climate of the Permian in Australia: the invertebrate faunas. *Palaeogeogr. Palaeoclimatol. Palaeoecol*., **23**, 33-46.

Dickens, J.M. (1996) Problems of a late Palaeozoic glaciation in Australia and subsequent climate in the Permian. *Palaeogeogr. Palaeoclimatol. Palaeoecol*., **125**, 185-197.

Eyles, C.H. and Eyles, N. (2000) Subaqueous mass flow origin for Lower Permian diamictites and associated facies of the Grant Group, Barbwire Terrace, Canning Basin, Western Australia. *Sedimentology*, **47**, 343-356.

Eyles, C.H., Eyles, N. and Gostin, V.A. (1998) Facies and allostratigraphy of high-latitude, glacially influenced marine strata of the Early Permian southern Sydney Basin, Australia. *Sedimentology*, **45**, 121-161.

Fielding, C.R., Naish, T.R., Woolfe, K.J. and Lavelle, M.A. (2000) Facies analysis and sequence stratigraphy of CRP-2/2A, Victoria Land Basin, Antarctica. *Terra Antartica*, **7**, 323-338.

Fielding, C.R., Naish, T.R. and Woolfe, K.J. (2001a) Facies architecture of the CRP-3 drillhole, Victoria Land Basin, Antarctica. *Terra Antartica*, **8**, 217-224.

Fielding, C.R., Sliwa, R., Holcombe, R.J. and Jones, A.T. (2001b) A new palaeogeographic synthesis for the Bowen, Gunnedah and Sydney Basins of eastern Australia. In: *Eastern Australasian Basins Symposium 2001: A Refocused Energy Perspective for the Future* (Eds. K.C. Hill and T. Bernecker), Petr. Explor. Soc. Austr. Spec. Publ., 269-278.

Forbes, D.L. and Boyd, R. (1987) Gravel ripples on the inner Scotian Shelf. *J. Sed. Petrol*., **57**, 46-54.

Gostin, V.A. and Herbert, C. (1973) Stratigraphy of the Upper Carboniferous and Lower Permian sequence, southern Sydney Basin. *J. Geol. Soc. Austr*., **20**, 49-70.

Holz, M. (2003) Sequence stratigraphy of a lagoonal estuarine system – an example from the lower Permian Rio Bonito Formation, Parana Basin, Brazil. *Sed. Geol*., **162**, 305-331.

Isbell, J.L., Miller, M.F., Wolfe, K.L., and Lenaker, P.A. (2003) Timing of Late Paleozoic glaciation in Gondwana: was glaciation responsible for the development of northern hemisphere cyclothems?, In: *Extreme Depositional Environments: Mega End Members in Geologic Time* (Eds. M.A. Chan and A.W. Archer), *Geol. Soc.Am. Spec. Pap*., **370**,5–24.

Jones, A.T. and Fielding, C.R. (2004) Sedimentological record of the Late Paleozoic glaciation in Queensland, Australia. *Geology*, **32**, 153-156.

Kidwell, S.M. (1984) Outcrop features and origin of basin margin unconformities in the Lower Chesapeake Group (Miocene), Atlantic coastal plain. In: *Interregional Unconformities and Hydrocarbon Accumulation* (Ed. J.S. Schlee), *AAPG Mem*., **36**, 37-58.

Kidwell, S.M. (1989) Stratigraphic condensation of marine transgressive records: origin of major shell deposits in the Miocene of Maryland. *J. Geol*., **97**, 1-24.

Kidwell, S.M. (1997) Anatomy of extremely thin marine sequences landward of a passive margin hinge-zone: Neogene Calvert Cliffs succession, Maryland, USA. *J. Sed. Res*., **67**, 322-340.

Lambeck, K. and Chappell, J. (2001) Sea level change through the last glacial cycle. *Science*, **292**, 679-686.

Larcombe, P. and Carter, R.M. (1998) Sequence architecture during the Holocene transgression: an example from the Great Barrier Reef shelf, Australia. *Sed. Geol*., **117**, 97-121.

Larcombe, P. and Carter, R.M. (2004) Cyclone pumping, sediment partitioning and the development of the Great Barrier Reef shelf system: a review. *Quat. Sci. Rev*., **23**, 107-136.

MacEachern, J. A., Bann, K. L., Bhattacharya, J. P. & Howell, C. D. (2005). Ichnology of deltas: organism responses to the dynamic interplay of rivers, waves, storms and tides. In: *River Deltas – Concepts, Models and Examples* (Eds: L. Giosan and J. Bhattacharya), *SEPM Spec. Publ.*, **83**, 49-85.

McHugh, C.M.G., Pekar, S.F., Christie-Blick, N., Ryan, W.B.F., Carbotte, S. and Bell, R. (2004) Spatial variations in a condensed interval between estuarine and open-marine settings: Holocene Hudson River estuary and adjacent continental shelf. *Geology*, **32**, 169-172.

Mifsud, J. (1990) *The Sedimentology and Diagenesis of the Upper Pebbley Beach Formation, Southern Sydney Basin*. B.Sc Honours Thesis, University of Wollongong (unbubl.).

Miller, K.G., Wright, J.D. and Fairbanks, R.G. (1991) Unlocking the Ice House: Oligocene-Miocene oxygen isotopes, eustasy and margin erosion. *J. Geophys. Res.*, **96**, 6829-6848.

Naish, T. and Kamp, P.J.J. (1997) Sequence stratigraphy of sixth-order (41 k.y.) Pliocene-Pleistocene cyclothems, Wanganui Basin, New Zealand: a case for the regressive systems tract. *Geol. Soc. Am. Bull*. **109**, 978-999.

Naish, T.R., Woolfe, K.J., Barrett, P.J., Wilson, G.S., Atkins, C., Bohaty, S.M., Bucker, C.J., Claps, M., Davey, F.J., Dunbar, G.B., Dunn, A.G., Fielding, C.R., Florindo, F., Hannah, M.J., Harwood, D.M., Henrys, S.A., Krissek, L.A., Lavelle, M.A., van der Meer, J., McIntosh, W.C., Niessen, F., Passchier, S., Powell, R.D., Roberts, A.P., Sagnotti, L., Scherer, R.P., Strong, C.P., Talarico, F., Verosub, K.L., Villa, G., Watkins, D.K., Webb, P-N. & Wonik, T. (2001) Orbitally induced oscillations in the East Antarctic ice sheet at the Oligocene/Miocene boundary. *Nature*, **413**, 719-723.

Posamentier, H.W. and Allen, G.P. (1999) *Siliciclastic Sequence Stratigraphy – Concepts and Applications*. SEPM Concepts in Sedimentology and Paleontology Series, **7**, 210pp.

Raychaudhuri, I., and Pemberton, S.G. (1992) Ichnologic and sedimentologic characteristics of open marine to storm dominated restricted marine settings within the Viking/Bow Island formations, south-central Alberta. In: *Application of Ichnology to Petroleum Exploration* (Ed. S.G. Pemberton), SEPM Core Workshop, **17**, 119-139.

Runnegar, B. (1979) Ecology of *Eurydesma* and the *Eurydesma* fauna, Permian of eastern Australia. *Alcheringa*, **3**, 261-285.

Saul, G., Naish, T.R., Abbott, S.T. and Carter, R.M. (1999) Sedimentary cyclicity in the marine Pliocene-Pleistocene of the Wanganui Basin (New Zealand): sequence stratigraphic motifs characteristic of the past 2.5 m.y. *Geol. Soc. Am. Bull*., **111**, 524-537.

Saunders, T.D.A., MacEachern, J.A., and Pemberton, S.G. (1994) Cadotte Member sandstone: progradation in a boreal basin prone to winter storms. In: *Canadian Society of Petroleum Geologists, Mannville Core Conference: CSPG Exploration Update* (Eds. S.G. Pemberton,, D.P. James, and D.M. Wightman), 331-349.

Schumm, S.A. and Ethridge, F.G. (1994) Origin, evolution and morphology of fluvial valleys. In: *Incised Valley Systems: Origin and Sedimentary Sequences* (Eds. R. Boyd, B. Dalrymple and B. Zaitlin), *SEPM, Spec. Publ*. **51**, 11-27.

Shanmugam, G., Poffenberger, M. and Toro Alava, J. (2000) Tide-dominated estuarine facies in the Hollin and Napo ("T" and "U") Formations (Cretaceous), Sacha Field, Oriente Basin, Ecuador. *AAPG Bull*., **84**, 652-682.

Takano, O. and Waseda, A. (2003) Sequence stratigraphic architecture of a differentially subsiding bay to fluvial basin: the Eocene Ishikari Group, Ishikari Coal Field, Hokkaido, Japan. *Sed. Geol*., **160**, 131-158.

Thomas, R.G., Smith, D.G., Wood, J.M., Visser, J., Calverley-Range, E.A. and Koster, E.H. (1987) Inclined Heterolithic Stratification – terminology, description, interpretation and significance. *Sed. Geol*., **53**, 123-179.

Tye, S.C. (1995) *Stratigraphy,Ssedimentology and Tectonic Significance of the Talaterang and Shoalhaven Groups in the Southern Sydney Basin*. PhD thesis, University of Wollongong (unpubl.).

Tye, S.C., Fielding, C.R. and Jones, B.G. (1996) Stratigraphy and sedimentology of the Permian Talaterang and Shoalhaven Groups in the southernmost Sydney Basin, New South Wales. *Austr. J. Earth Sci*., **43**, 57-69.

Van Wagoner, J.C., Mitchum, R.M. Jr., Campion, K.M. and Rahmanian, V.D. (1990) Siliciclastic sequence stratigraphy in well logs, core and outcrops: concepts for high-resolution correlation of time and facies. *AAPG Methods in Exploration Series* **7**, 55pp.

Van Wagoner, J.C., Jones, C.R., Taylor, D.R., Nummedal, D., Jennette, D.C. and Riley, G.W. (1991) *Sequence Stratigraphy: Applications to Shelf Sandstone Reservoirs, AAPG Field Conference, September 21-28, 1991, Guidebook.*

Veevers, J.J. and Powell, C. McA. (1987) Late Paleozoic glacial episodes in Gondwanaland reflected in transgressive-regressive depositional sequences in Euramerica. *Geol. Soc. Am. Bull*., **98**, 475-487.

Walker, R.G. and Plint, A.G. (1992) Wave- and storm-dominated shallow marine systems. In: *Facies Models: Response to Sea Level Change* (Eds. R.G. Walker and N.P. James), Geol. Assoc. Can., St John's, 219-238.

Zachos, J., Pagani, M., Sloan, L., Thomas, E. and Billups, K. (2001) Trends, rhythms and aberrations in global climate 65 Ma to present. *Science*, **292**, 686-693.

Zaitlin, B.A., Dalrymple, R.W. and Boyd, R. (1994) The stratigraphic organization of incised-valley systems associated with relative sea-level change. In: *Incised Valley Systems: Origin and Sedimentary Sequences* (Eds. R. Boyd, B. Dalrymple and B. Zaitlin), SEPM, Spec. Publ. **51**, 45-62.

TABLE AND FIGURE CAPTIONS

Table 1 – Characteristics of Facies Associations A and B. The facies scheme is an extended version of that presented in Bann *et al*., 2004.

Figure 1 – Maps showing the location of the study area in Australia, the Permo-Triassic Bowen-Gunnedah-Sydney Basin system in eastern Australia, the location of the study area at the southernmost onshore limit of the Sydney Basin, and the location of specific outcrops utilized in the study.

Figure 2 – Stratigraphic framework diagram for the Talaterang and Shoalhaven Groups of Permian age in the southern Sydney Basin with underlying tectonic context, and highlighting the west to east lithological variations in the interval of interest (modified from Tye *et al*., 1996). Abbreviations: St'mak – Sterlitamakian, Art. – Artinskian, Kun. – Kungurian, Ufim. – Ufimian, N-m – Non-marine, Y.C.M. – Yarrunga Coal Measures.

Figure 3 – Palaeogeographic map of the Bowen-Gunnedah-Sydney Basin System (BGSBS) during mid Early Permian (Sakmarian-Artinskian) times, showing the formation of a north-south-elongate seaway by amalgamation of numerous, previously discrete, extensional basins (from Fielding *et al*., 2001b). Isolated outcrop areas of marine facies of this age to the east of the basin system, within the fold-thrust belt formed during the later Hunter-Bowen Contractional Event, suggest that the. BGSBS may have been open (or at least connected) to the palaeo-Pacific

Ocean during the middle Early Permian. The study area is in the far south of the (onshore) basin system, on the south coast of New South Wales (NSW). QLD – Queensland.

Figure 4 – Photographs of Facies A1 and A2 (Lower and Upper Offshore, respectively). A) general view of the interval 20-22 m at Clear Point (Figure 15), showing heterolithic estuarine channel fill (Facies B8) at base, abruptly overlain across a Transgressive Surface of Erosion by bioturbated mudrocks of Facies A1 (Lower Offshore, interval arrowed), in turn truncated by an abrupt contact (Sequence Boundary) that is overlain by cross-bedded sandstone of Facies B8 (Estuarine Channel). B) detail of bioturbated sandy siltstone (Facies A1) at Mill Point, containing a distal expression of the *Cruziana* Ichnofacies composed of *Rosselia socialis (Rs), Cosmorhaphe (Cr), Planolites (P), Zoophycos (Z), Phycosiphon (Ph)* and *Diplocraterion habichi (Dh)*. C) close-up view of same exposure as in B), showing distal expression of the *Cruziana* ichnofacies. As – *Asterosoma*, Ch – *Chondrites*, P – *Planolites*, Ph – *Phycosiphon*.

Figure 5 – Photographs of Facies A3 (Offshore Transition). A) general view of Facies A3 at Mill Point. B) detail of bedding structure partially destroyed by bioturbation at Clear Point. C) close-up of mixed, diverse *Skolithos-Cruziana* ichnofacies in Facies A3 at Clear Point. Ch – *Chondrites*, P – *Planolites*, Ph – *Phycosiphon*, Si – *Siphonichnus*.

Figure 6 – Photographs of Facies A4 (Distal Lower Shoreface) and A5 (Proximal Lower Shoreface). A) General view of Facies A5 showing Hummocky Cross-Stratified sandstones (Facies A5) with complete preservation of hummock bedform (arrowed interval 20 cm) capped by large, gravelly, symmetrical ripples, and overlying bioturbated sandstones (Facies A4) at Mill

Point. Dh – *Diplocraterion habichi*. B) detail of Facies A4 and A5 at Mill Point, showing bioturbated intervals, low-angle cross-bedding (Hummocky Cross-Stratification?), unidirectional cross-bedding and symmetrical wave ripple-topped beds. Sandstone tempestites display a *Skolithos* ichnofacies, whereas interbedded finer-grained intervals show a *Cruziana* ichnofacies. Dh – *Diplocraterion habichi*, Rr – *Rosselia rotatus*. Scale bar is 15 cm. C) detail of bed geometry and internal structure in Facies A4 and A5 at Mill Point. Hummocky Cross-Stratified bed indicated by arrowed interval (20 cm), white arrow shows scour surface overlain by cross-bedded sandstone lens. D) close-up of internal structure of Facies A5, showing bioturbated intervals, hummocky cross-stratification, small-scale symmetrical wave ripples (white arrows) and large, gravelly, symmetrical ripples (black arrow) at Mill Point. Unbioturbated mud drapes over ripple forms suggest a deltaic influence on sedimentation (see text). Scale bar is 15 cm. D) Close-up of internal structure shown in B), showing *Skolithos*-*Cruziana* ichnofacies, and large, gravelly, symmetrical ripples (black arrows) with overlying sparsely bioturbated mud drapes. Rr – *Rosselia rotatus*, Te – *Teichichnus*.

Figure 7 – Photographs of Facies A7 (Transgressive Sand Sheets). A) general view at Clear Point, showing lower, heavily bioturbated interval (short arrowed interval: 40 cm), with a *Glossifungites* Ichnofacies-demarked surface at the base, overlain by more sparsely bioturbated, cross-bedded sandstone. The total vertical extent of the facies is indicated by the long arrowed line. B) general view of Facies A7 at Mill Point, showing strongly bioturbated sandstone overlying dark grey mudrocks with loaded sandstone lenses of Facies B10. The basal surface of Facies A7 is demarked by a *Glossifungites* ichnofacies assemblage. C) close-up of bioturbation

typical of the cross-bedded variant of Facies A7. Cy – *Cylindrichnus*, Dh – *Diplocraterion habichi*, S – *Skolithos*.

Figure 8 – Photographs of Facies B1 (Heterolithic, Estuarine Channel Fills). A) general view of extensive channel fill at Point Upright. The basal erosion surface, with c. 6 m relief, overlies Facies A4 and A5 and is interpreted as a Sequence Boundary. The channel fill in the foreground displays Inclined Heterolithic Stratification (IHS), whereas the concentric channel in the distance is composed of Facies B10. Elements of intrasets can be seen within some of the inclined stratification. B) detail of the uppermost part of the channel fill at Point Upright, showing truncation of Facies B1 by Facies B10. Interval shown is c. 3 m. C) close-up of small-scale sedimentary structure within heterolithic sandstone siltstone of Facies B1 at Clear Point, showing bidirectional current ripple cross-lamination, wave-modified current ripple cross-lamination, synaeresis cracks (sy) and plant debris (white arrows).

Figure 9. Photographs of Facies B2 (Coastal Basin Fills). A) general view of flat-bedded, heterolithic Facies B2 abruptly overlying Facies A2 across a Sequence Boundary (Kerrie's knee height) at Point Upright. B) close-up of sedimentary structure, showing ripple cross-lamination (cr) with rhythmic alternation of sand and mud laminae. C) close-up of low diversity bioturbation in Facies B2 at Mill Point, showing *Planolites* (P) and *Thalassinoides* (Th). D) close-up of rhythmic alternation of planar laminated fine sandstone and siltstone (beneath scale bar), interpreted as tidal basin rhythmites.

Figure 10 – Photographs of Facies B3 (Toxic/Anoxic Coastal Channel and Basin Fills). A) general view of concentric mudstone-filled channel at Point Upright (see also Fig. 8A). The channel base is cut into shoreface sandstones (Facies A4/A5) and constitutes a Sequence Boundary. B) Detail of the channel base as above, showing pebble lag along the basal erosion surface. C) close-up of sparse bioturbation in Facies B3, mainly *Planolites* (P) which form part of a *Glossifungites* ichnofacies assemblage subtending from the overlying sandstone.

Figure 11 – Photographs and split core diagram of key surfaces in the upper Pebbley Beach. A) combined Sequence Boundary/Flooding Surface (SB/FS) at Mill Point (c. 16.5 m on Fig. 15) separating Facies A1 (Lower Offshore:LOS) below from Facies B2 (Estuarine Basin: EB) above. Note the fine gravel-filled *Conichnus* along the contact, demarking a *Glossifungites* ichnofacies assemblage, and the *Lingulichnus* equilibrium adjustment (ea) structures that cross the boundary between the two facies. B) combined Sequence Boundary/Flooding Surface (SB/FS: arrowed) at Clear Point (c. 20 m on Fig. 16) separating Facies A3 (Offshore Transition: OST) below from Facies B1 (Estuarine Channel: EC) above. Note the *Diplocraterion habichi* (D) that define a palimpsest assemblage along the contact. C) Transgressive Surface of Erosion (TSE) at Mill Point (c. 7-8 m on Fig. 15), separating Facies B2 (Estuarine Basin: EB) below from Facies A5 (Proximal Lower Shoreface: LSF) above. Note the intense soft-sediment deformation of the contact. D) combined Sequence Boundary/Flooding Surface (SB/FS) at Point Upright (c. 5-6 m on Fig. 14) separating Facies A4 (Distal Lower Shoreface: LSF) below from Facies B3 (Abandoned Estuarine Channel Fill:EA) above. Note the *Diplocraterion habichi* along the contact (arrowed), demarking a *Glossifungites* ichnofacies assemblage. E) split core diagram illustrating trace fossil assemblages across a combined Sequence Boundary/Flooding Surface

(FS/SB) at Mill Point (xx-xx m on Figure 15). The lower part of the diagram illustrates an archetypal *Cruziana* Ichnofacies characteristic of Lower Offshore facies (A1), while the upper part of the diagram shows a stressed expression of the *Cruziana* Ichnofacies characteristic of Estuarine Basin deposits (Facies B2). Note the presence of gravelly sandstone-filled burrows subtending from the contact between the two facies, demarking a *Glossifungites* Ichnofacies assemblage (*GI*). Abbreviations: ea – equilibrium adjustment structures, *Rs – Rosselia socialis, Te – Teichichnus, P – Planolites, L – Lingulichnus, Th – Thalassinoides*, Sy – synaeresis cracks, *C – Conichnus, Cy – Cylindrichnus, Pa – Palaeophycus heberti, Rh – Rhizocorallium, Cr – Cosmorhaphe, Ts – Taenidium synyphes, Z – Zoophycos, H – Helminthopsis, Pt – Palaeophycus tubularis, Ch – Chondrites, Ph – Phycosiphon, As – Asterosoma*.

Figure 12– Photograph, palaeocurrent data and interpretive map of channel fills (Facies B1 and B3) at Point Upright. The most southerly channel shows evidence of lateral accretion to the east and palaeoflow to the southwest and east, while the external and internal geometry of a smaller pair of channels exposed to the north is suggestive of a downstream-bifurcating channel system.

Figure 13– Photomosaic of the southwest face of Mill Point (red arrows on location map), showing the complex architecture of the interval around 15 – 20 m on Figure 15, scale drawing of the entire face showing subdivision of channel fill facies (B1 and B3) into four discrete generations of channels (1-4), and the palaeocurrent data from each of these four generations. The composite, multi-storey/multi-lateral channel body abruptly overlies a persistent erosion surface interpreted as a Sequence Boundary, which truncates shoreface (A4-A6) and other open marine facies. The sequence architecture in this part of the succession is considered to be highly

condensed and truncated. Thin lenses of Facies A1 – A3 are locally preserved between individual channel bodies, suggesting that each channel generation may record a separate sequence. Generation 1 channel fill is coarse-grained, pebbly, trough cross-bedded sandstone (Facies B1a), and may record Lowstand Systems Tract deposition. LSF – Lower Shoreface, OS – Offshore, EB – Estuarine Basin, EC – Estuarine Channel, SB – Sequence Boundary, FS – Flooding Surface, TSE – Transgressive Surface of Erosion.

Figure 14 – A) Composite, graphic sedimentological log of the section exposed at Point Upright. The laterally restricted estuarine channel fill shown to the right of the log cuts down from c. 6.5 m (see Figure 12). B) key to symbols used in Figures 14-18. BI – Bioturbation Index.

Figure 15 – Composite, graphic sedimentological log of the section exposed at Mill Point. See Figure 14 for key to symbols used. Of the two laterally restricted estuarine channel fills shown to the right of the log, the lower one cuts down from the Sequence Boundary at c. 15 m, and the upper one from the Sequence Boundary at c. 22 m.

Figure 16 – Composite, graphic sedimentological log of the section exposed at Clear Point. See Figure 14 for key to symbols used.

Figure 17 – Cross-section illustrating the detailed correlation of sections from Point Upright in the south to Clear Point in the north, and highlighting the preservation of isolated channel fills at various stratigraphic horizons. Note, however, the lateral continuity of every key surface and sequence recognized. See Figure 14 for key to symbols used. Sequences 1-9 are as in Figure 18.

Figure 18– Composite, graphic sedimentological log of the entire upper Pebbley Beach Formation, showing every interval at its maximum vertical thickness recorded at outcrop, together with sedimentological and trace fossil data, the sequence stratigraphic subdivision of the section, and an interpreted relative sea-level curve. Note the thin, strongly condensed, incomplete and top-truncated nature of sequences within this section. See Figure 14 for key to symbols used.

Table 1

Association/ facies	Lithology	Primary structures	Ichnofacies	Interpretation
A1	Thoroughly bioturbated siltstone with rare, thin, fine-grained sandstone laminae and beds	Little primary structure preserved. Undulatory lamination, combined flow ripple cross-lamination and possible HCS in sandstones, glendonites, outsized clasts, plant debris	Diverse, distal *Cruziana*	Lower offshore
A2	Thoroughly bioturbated, sandy siltstone, with rare but increasing fine-grained sandstone beds	As for A1	Diverse, Archetypal *Cruziana*, with elements of *Skolithos* in sandstones	Upper offshore
A3	Interbedded bioturbated sandy siltstone and laminated sandstone	Some parts display little primary structure, others preserve laminated to burrowed fabric (Lam-Scram) with HCS, low-angle planar lamination, wave and combined-flow ripple cross-lamination, synaeresis cracks, outsized clasts, plant debris, shell fossils	Mixed, diverse *Skolithos–Cruziana*	Offshore transition, possible deltaic influences
A4	Thoroughly bioturbated muddy sandstone	As for A3	Proximal *Cruziana* + minor *Skolithos*	Distal lower shoreface water depths on wave-dominated delta front
A5	Interbedded laminated sandstone, bioturbated muddy sandstone and dark claystone, minor conglomerate	As for A3, plus large, gravelly, symmetrical ripples, claystones show synaeresis cracks	Proximal *Cruziana*	Proximal lower shoreface water depths on wave-dominated delta front
A6	Amalgamated, laminated sandstone, minor conglomerate	Gravel lags, large-scale HCS, low-angle and flat lamination, symmetrical and interference ripples, large gravelly symmetrical ripples	Archetypal *Skolithos* + minor *Cruziana*	Middle shoreface water depths on wave-dominated delta front
A7	Bioturbated, laterally variable sandstone	HCS, trough cross-bedding with mud partings on foresets, small-scale and large gravelly symmetrical ripples, shell and plant debris	Distal *Skolithos*	Transgressive sand sheets
B1	Channelized, heterolithic sandstone-mudstone, some bodies with basal storey of coarse-grained, cross-bedded sandstone (Facies B1a)	Channel forms, basal gravel lags, inclined heterolithic stratification, cross-bedding, ripple cross-lamination, linsen, lenticular, wavy and flaser bedding, mud drapes, rhythmic sand-mud couplets, graded sandstone beds, synaeresis cracks, convolute bedding, abundant plant debris	Very restricted, mixed *Skolithos–Cruziana*	Mixed-load fill of sinuous estuarine channels
B2	Sheet-like, heterolithic sandstone-mudstone	Current and wave-modified current ripple cross-lamination, micro-HCS, linsen, lenticular, wavy and flaser bedding, mud drapes, rhythmic sand-mud couplets, synaeresis cracks, minor soft-sediment deformation	Highly stressed *Cruziana*	Protected, wave- and tidally-influenced coastal basins
B3	Laminated to blocky, dark grey mudstone	Channel forms, linsen-laminated or normally graded sandstone laminae	None	Suspended load fill of estuarine channels and basins (toxic and/or anoxic)

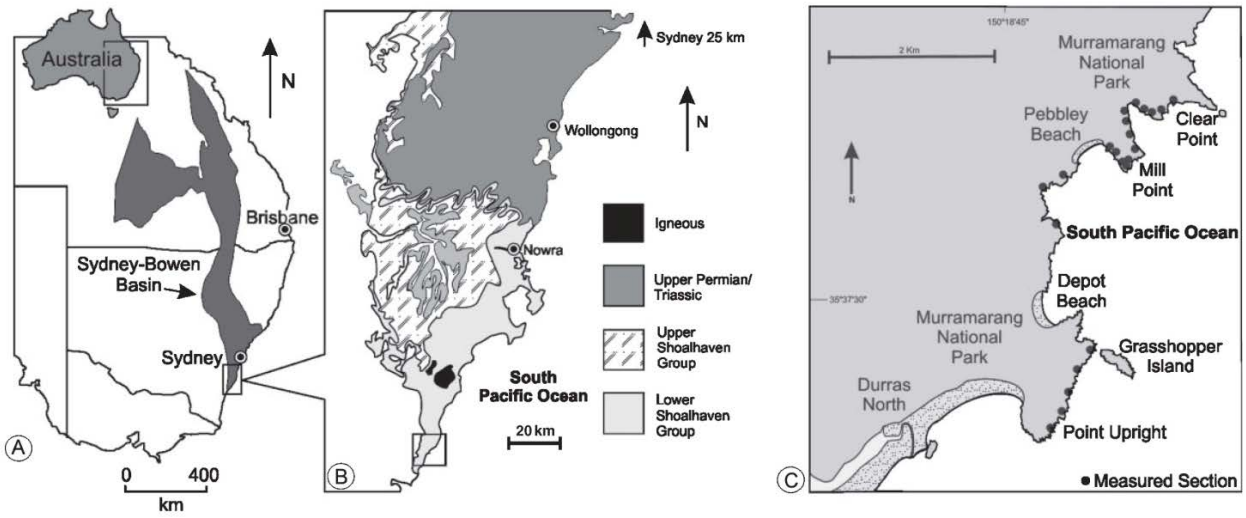

Figure 1

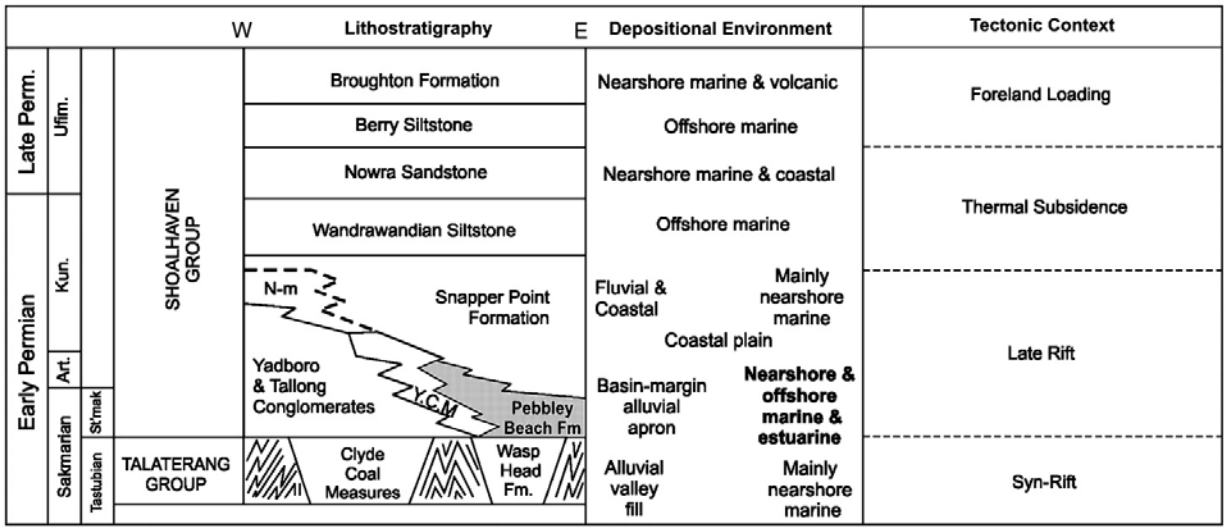

Figure 2

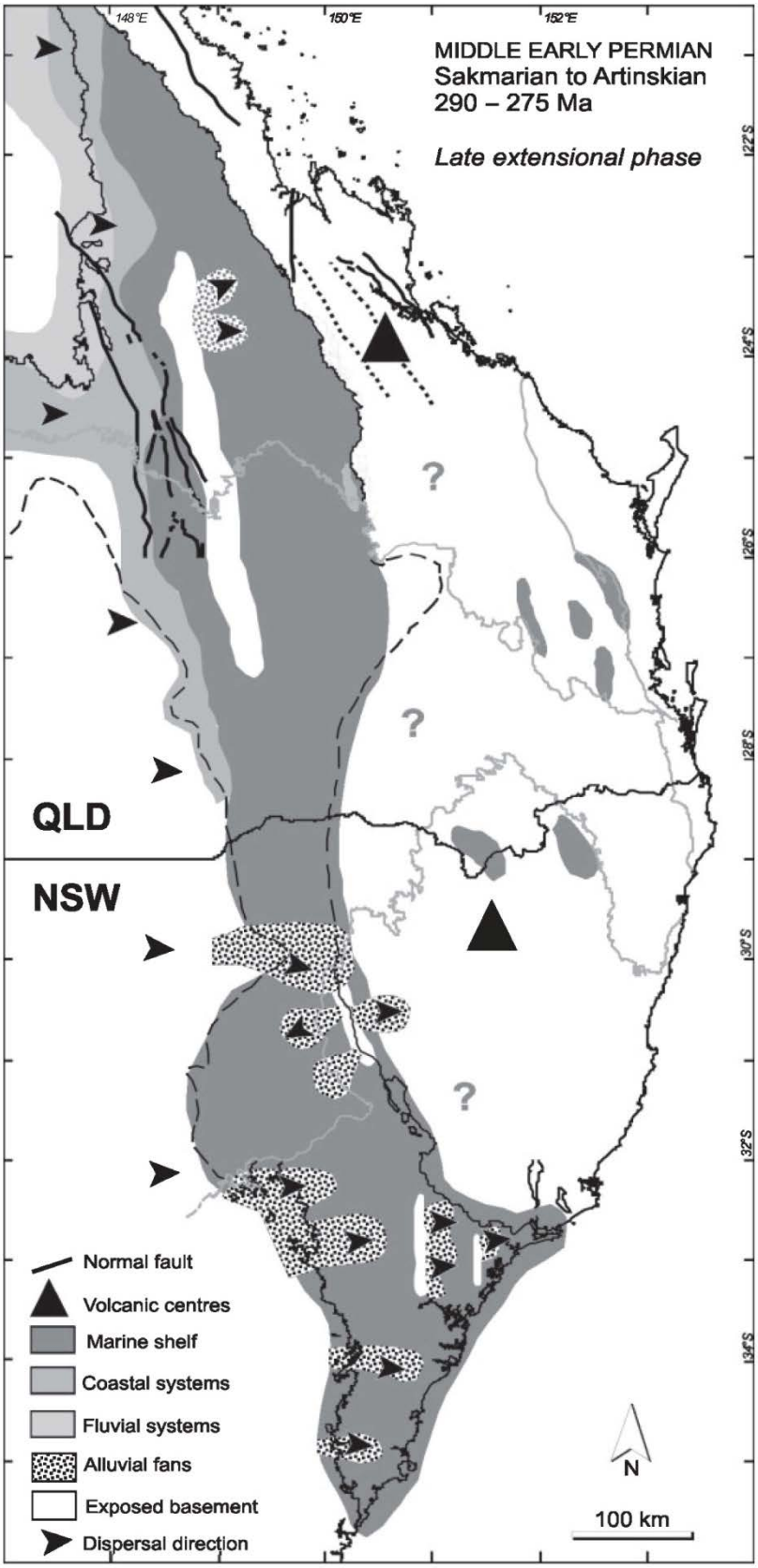
148°E
150°E
152°E
MIDDLE EARLY PERMIAN
Sakmarian to Artinskian
290 – 275 Ma
Late extensional phase
122°S
124°S
126°S
128°S
130°S
132°S
134°S
QLD
NSW
?
?
?
Normal fault
Volcanic centres
Marine shelf
Coastal systems
Fluvial systems
Alluvial fans
Exposed basement
Dispersal direction
N
100 km

Figure 3

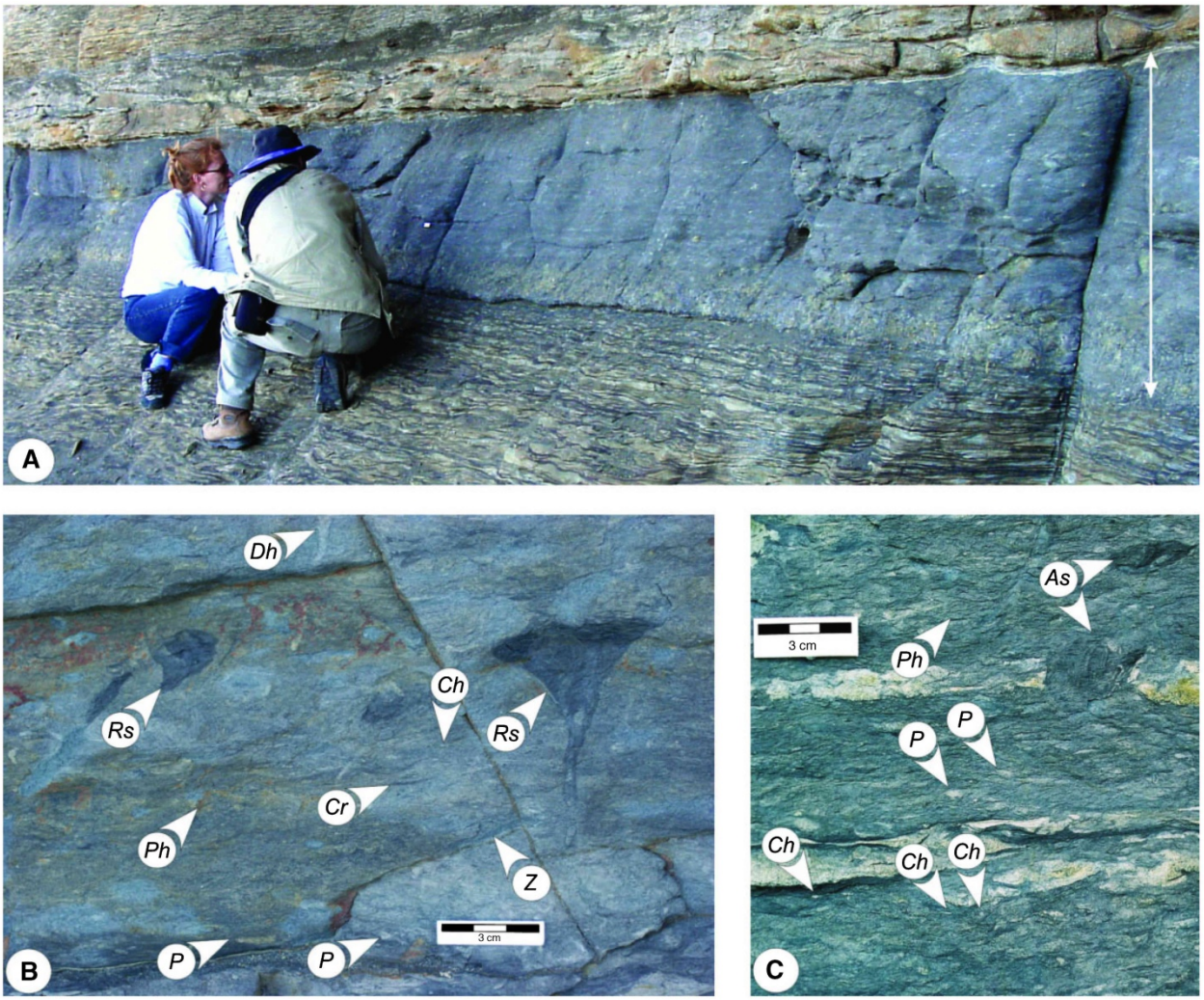

Figure 4

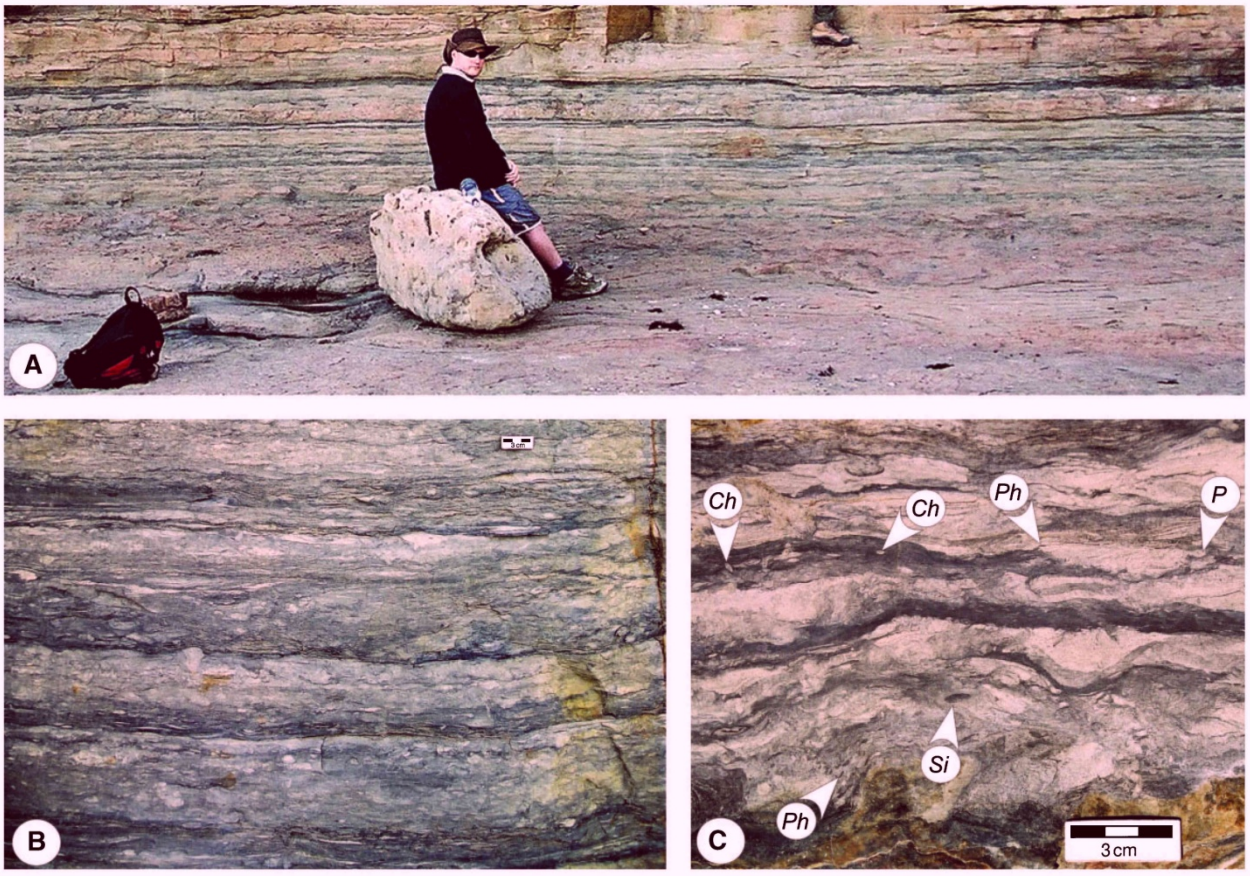

Figure 5

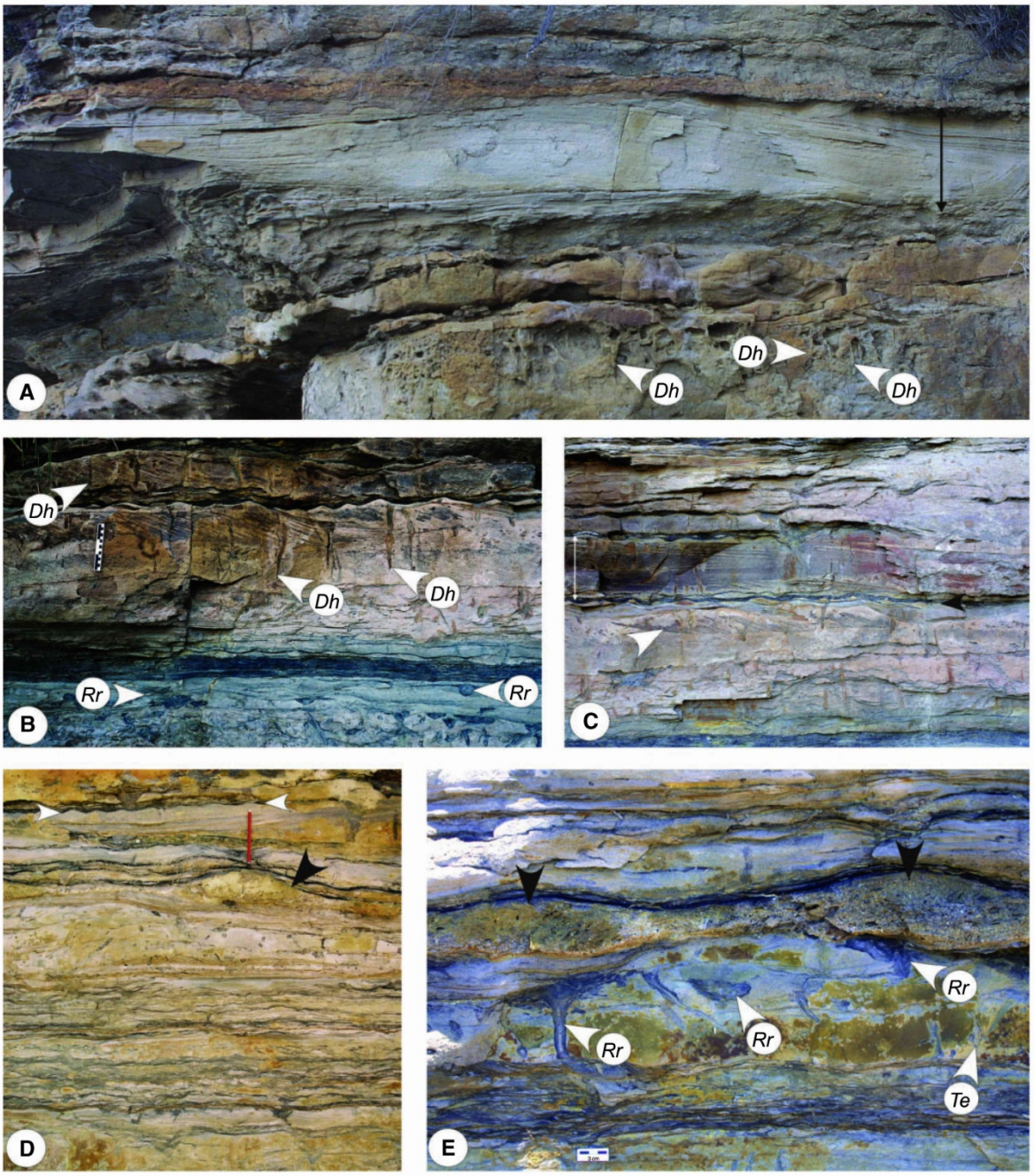

Figure 6

Figure 7

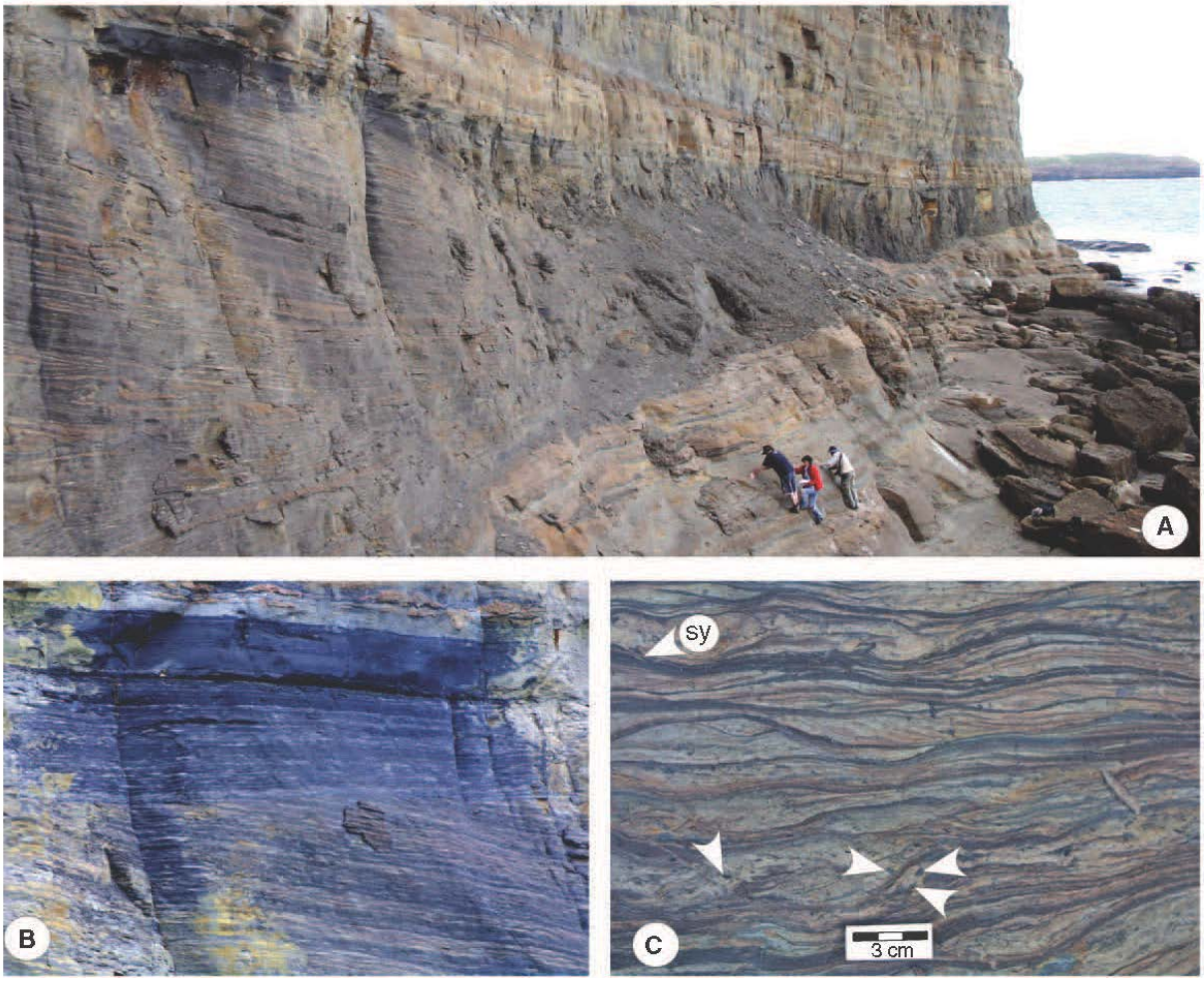

Figure 8

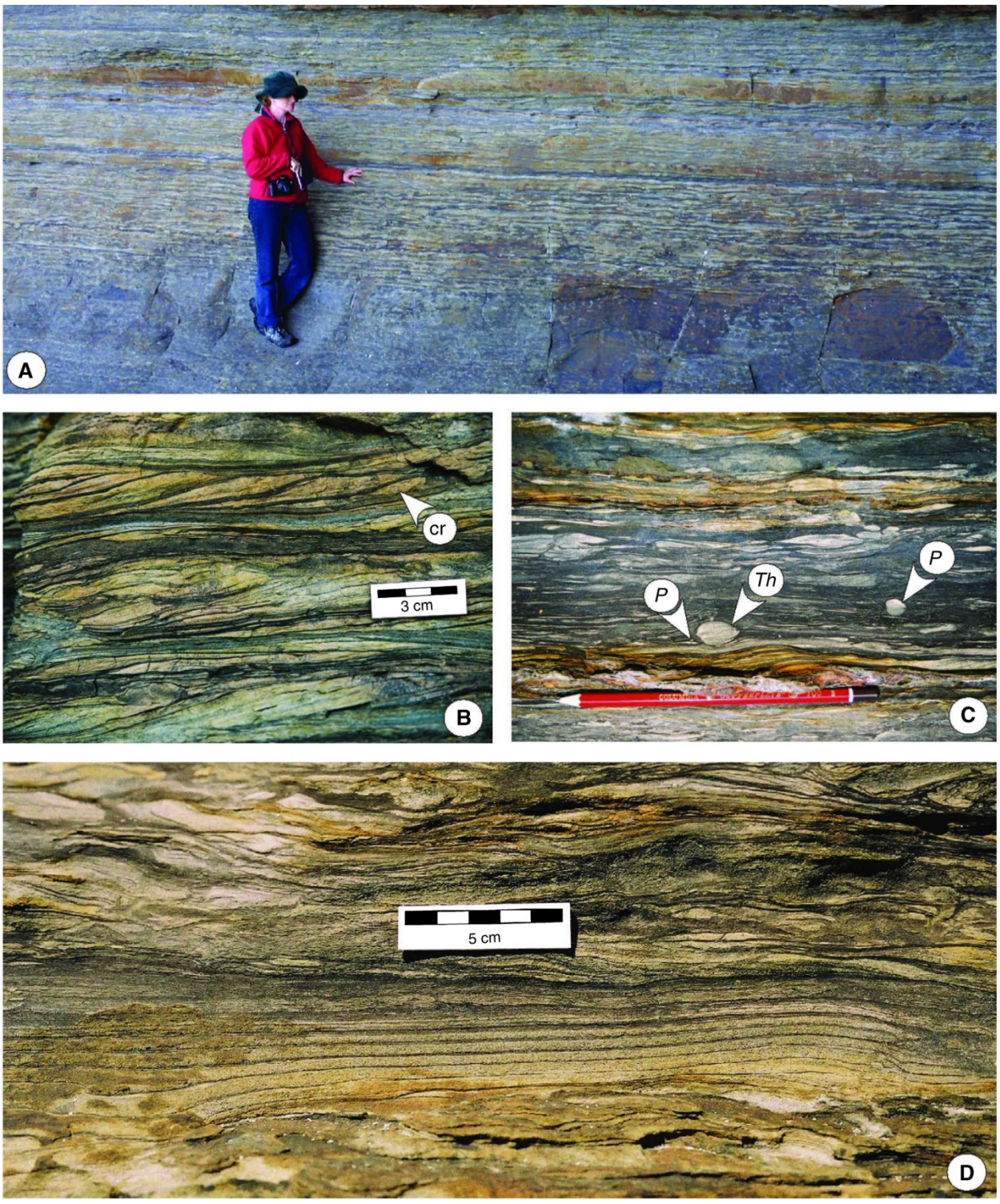

Figure 9

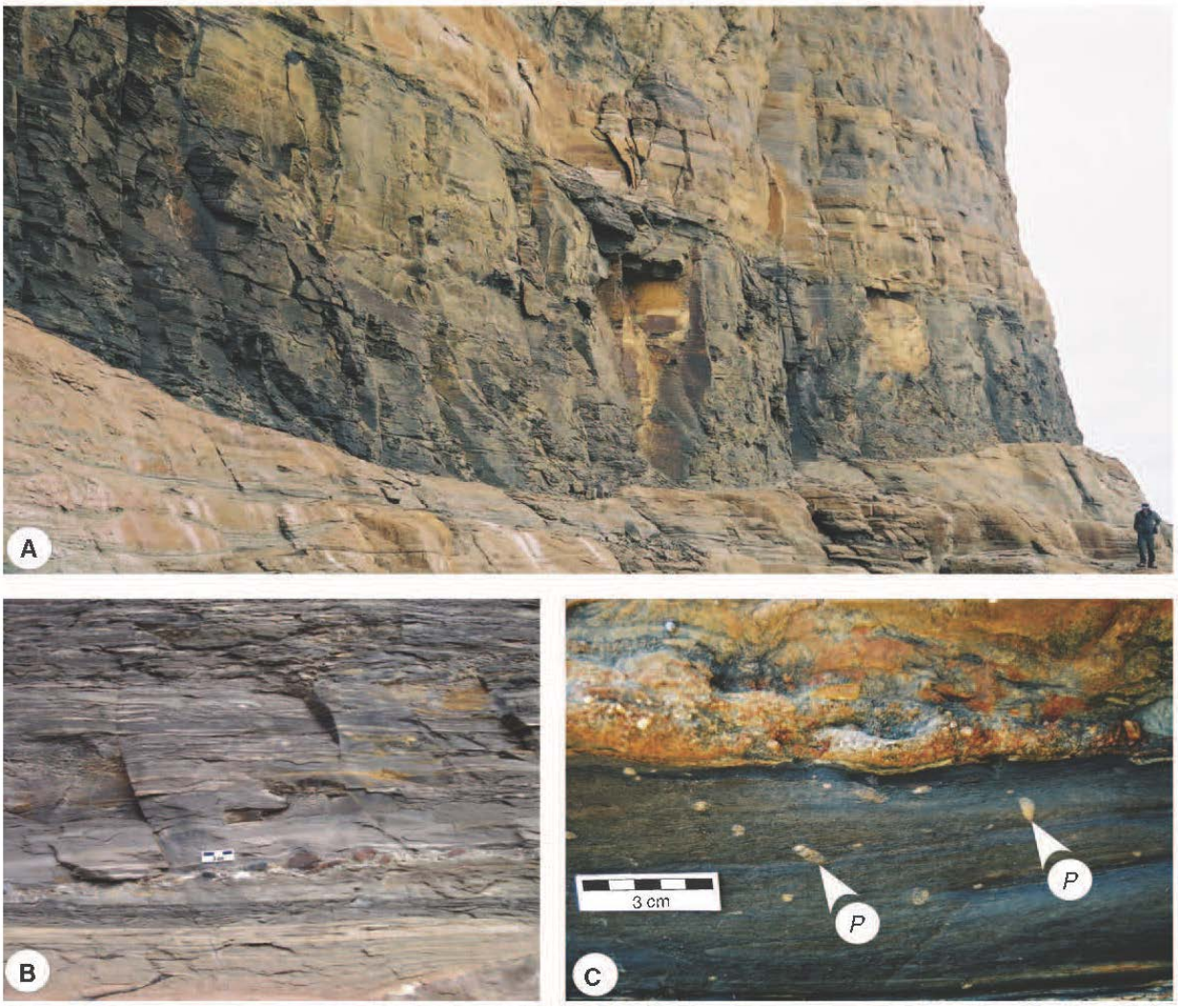

Figure 10

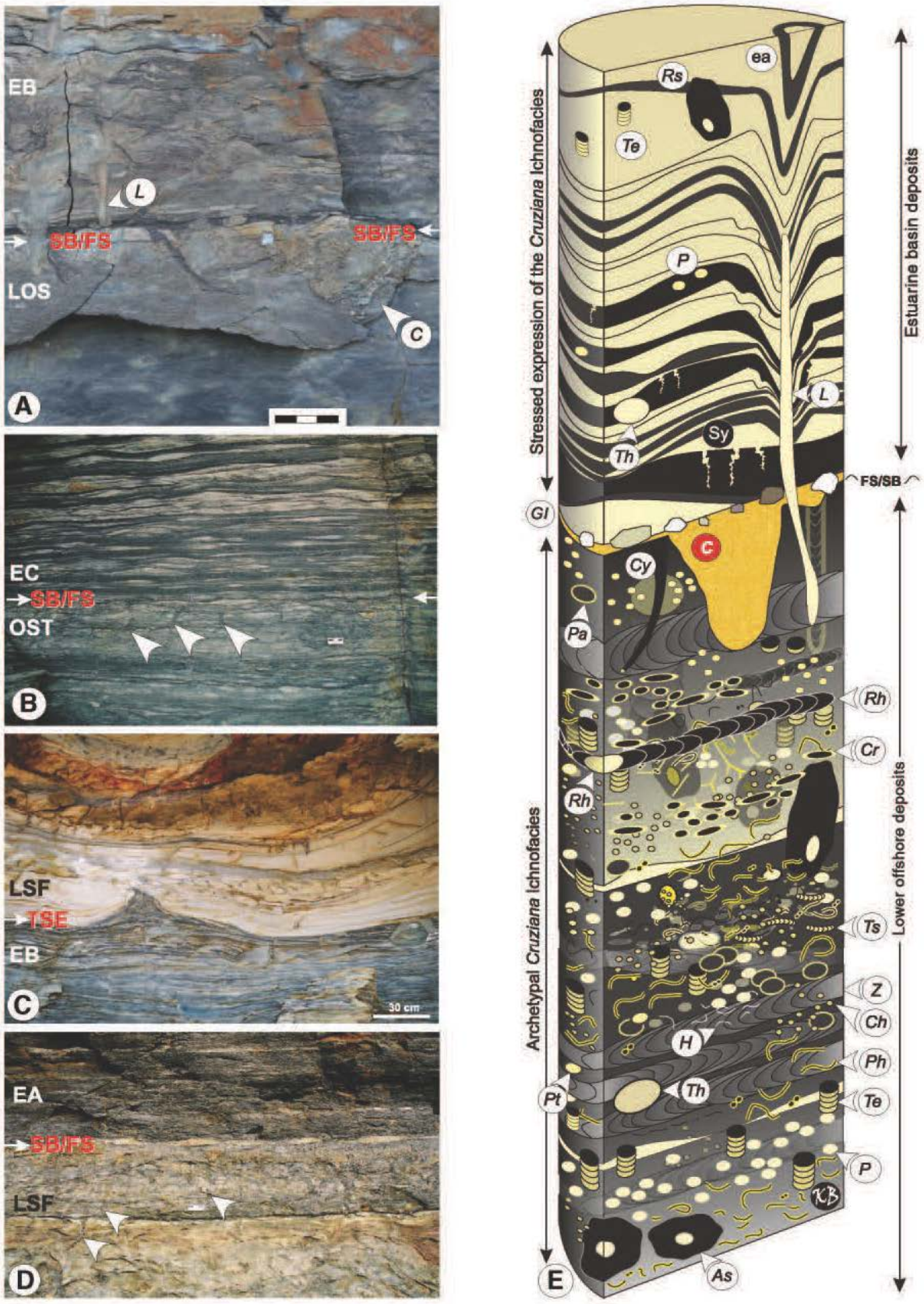
EB
L
SB/FS
SB/FS
LOS
C
A
EC
SB/FS
OST
B
LSF
TSE
EB
30 cm
C
EA
SB/FS
LSF
D
Stressed expression of the Cruziana Ichnofacies
Archetypal Cruziana Ichnofacies
Estuarine basin deposits
Lower offshore deposits
ea
Rs
Te
P
L
Sy
Th
FS/SB
Gl
C
Cy
Pa
Rh
Cr
Rh
Ts
Z
Ch
H
Ph
Pt
Th
Te
P
KB
As
E

Figure 11

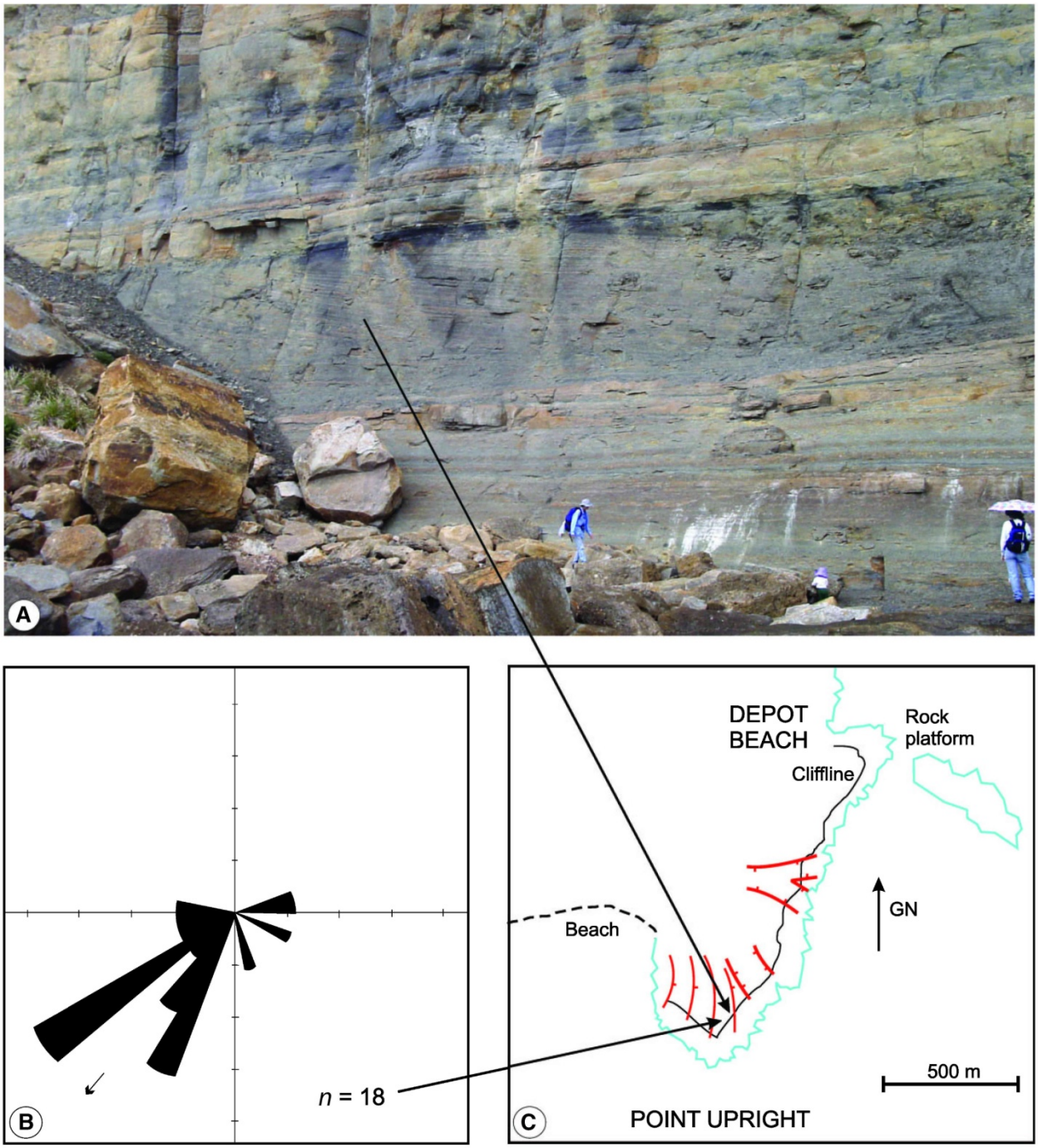
A
B
n = 18
C
DEPOT
BEACH
Rock
platform
Cliffline
Beach
GN
500 m
POINT UPRIGHT

Figure 12

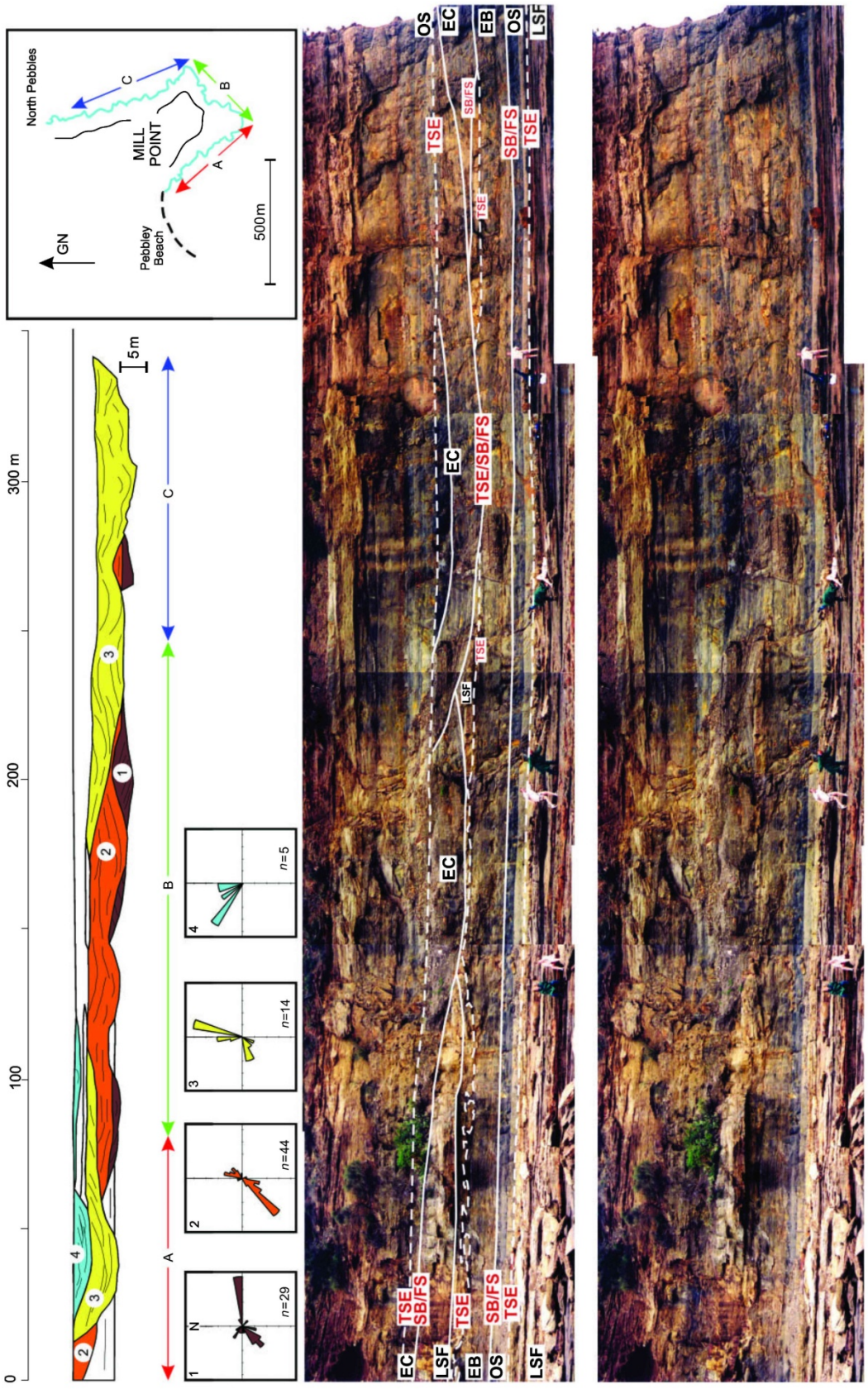
North Pebbles
MILL POINT
Pebbley Beach
GN
500m
A
B
C
0
100
200
300 m
5 m
n=29
n=44
n=14
n=5
TSE
SB/FS
EC
LSF
EB
OS
TSE/SB/FS

Figure 13

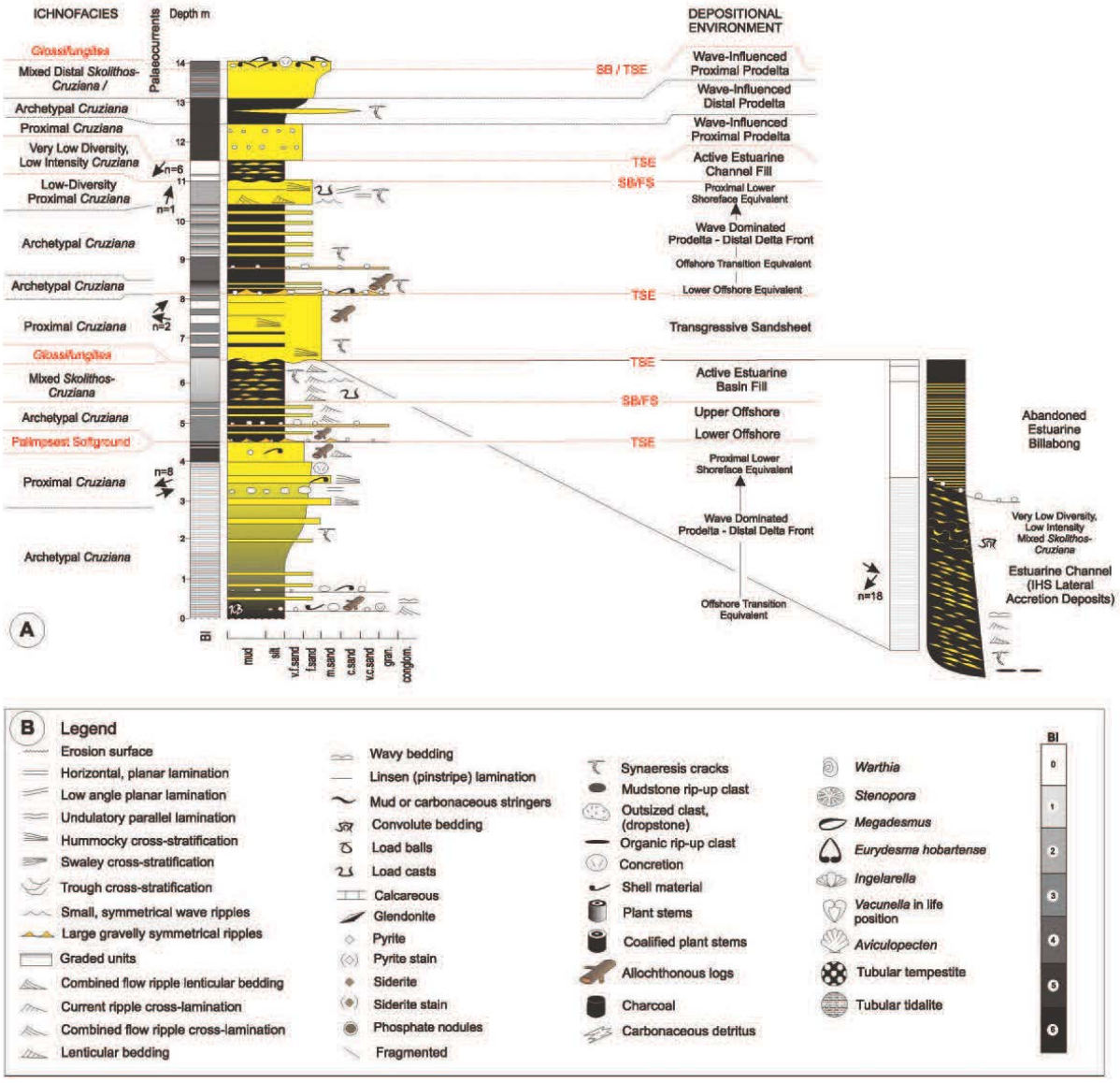
ICHNOFACIES
Depth m
Palaeocurrents
DEPOSITIONAL ENVIRONMENT
Glossifungites
Mixed Distal Skolithos-Cruziana /
Archetypal Cruziana
Proximal Cruziana
Very Low Diversity, Low Intensity Cruziana
Low-Diversity Proximal Cruziana
Archetypal Cruziana
Archetypal Cruziana
Proximal Cruziana
Glossifungites
Mixed Skolithos-Cruziana
Archetypal Cruziana
Palimpsest Softground
Proximal Cruziana
Archetypal Cruziana
n=6
n=1
n=2
n=8
SB / TSE
TSE
SB/FS
TSE
TSE
SB/FS
TSE
Wave-Influenced Proximal Prodelta
Wave-Influenced Distal Prodelta
Wave-Influenced Proximal Prodelta
Active Estuarine Channel Fill
Proximal Lower Shoreface Equivalent
Wave Dominated Prodelta - Distal Delta Front
Offshore Transition Equivalent
Lower Offshore Equivalent
Transgressive Sandsheet
Active Estuarine Basin Fill
Upper Offshore
Lower Offshore
Proximal Lower Shoreface Equivalent
Wave Dominated Prodelta - Distal Delta Front
Offshore Transition Equivalent
n=18
Abandoned Estuarine Billabong
Very Low Diversity, Low Intensity Mixed Skolithos-Cruziana
Estuarine Channel (IHS Lateral Accretion Deposits)
BI
mud
silt
v.f.sand
f.sand
m.sand
c.sand
vc.sand
gran.
conglom.
A
B
Legend
Erosion surface
Horizontal, planar lamination
Low angle planar lamination
Undulatory parallel lamination
Hummocky cross-stratification
Swaley cross-stratification
Trough cross-stratification
Small, symmetrical wave rippies
Large gravelly symmetrical ripples
Graded units
Combined flow ripple lenticular bedding
Current ripple cross-lamination
Combined flow ripple cross-lamination
Lenticular bedding
Wavy bedding
Linsen (pinstripe) lamination
Mud or carbonaceous stringers
Convolute bedding
Load balls
Load casts
Calcareous
Glendonite
Pyrite
Pyrite stain
Siderite
Siderite stain
Phosphate nodules
Fragmented
Synaeresis cracks
Mudstone rip-up clast
Outsized clast, (dropstone)
Organic rip-up clast
Concretion
Shell material
Plant stems
Coalified plant stems
Allochthonous logs
Charcoal
Carbonaceous detritus
Warthia
Stenopora
Megadesmus
Eurydesma hobartense
Ingelarella
Vacunella in life position
Aviculopecten
Tubular tempestite
Tubular tidalite
BI
0
1
2
3
4
5
6

Figure 14

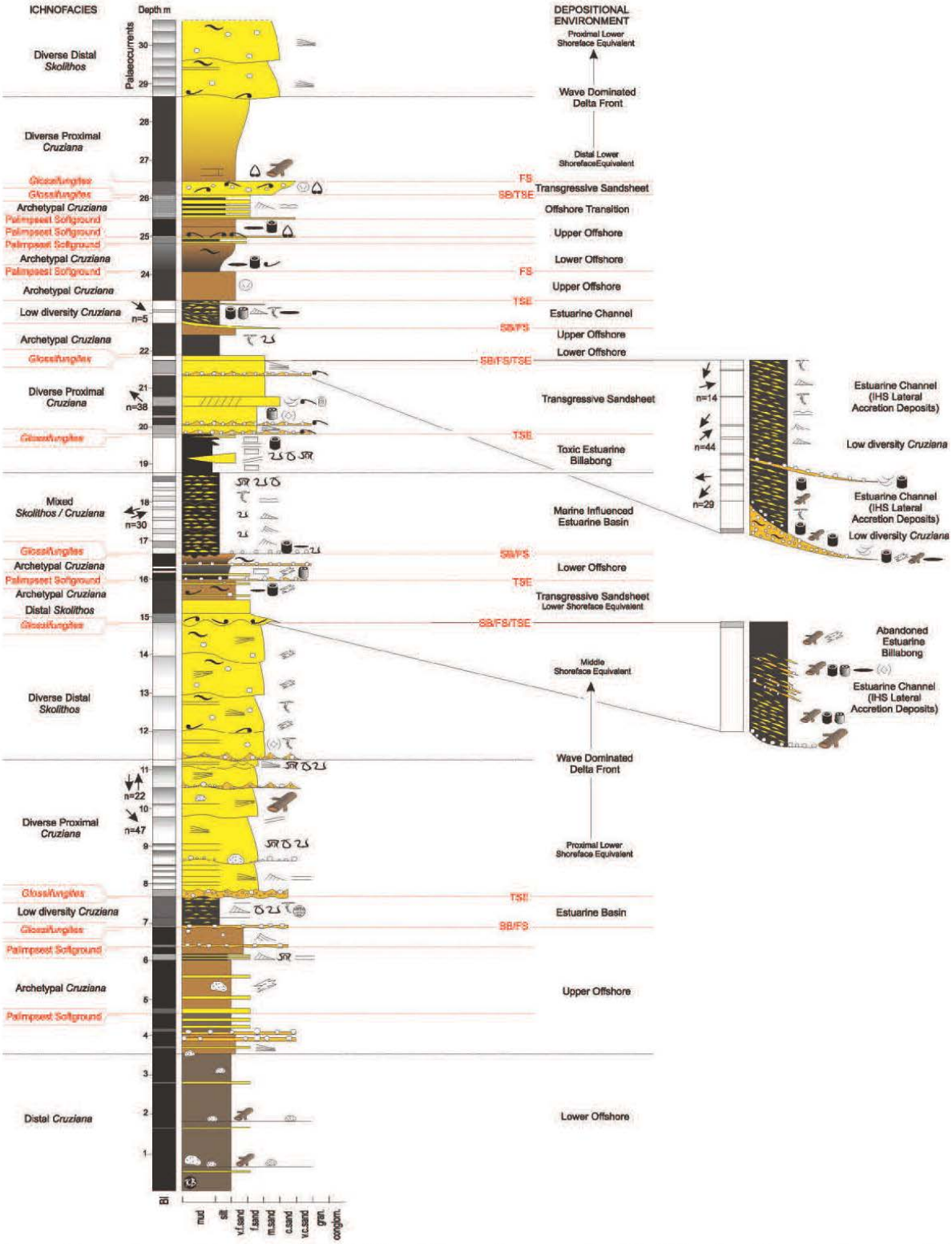
ICHNOFACIES
Depth m
Palaeocurrents
DEPOSITIONAL ENVIRONMENT
Proximal Lower Shoreface Equivalent
Wave Dominated Delta Front
Distal Lower ShorefaceEquivalent
Diverse Distal Skolithos
Diverse Proximal Cruziana
Glossifungites
Archetypal Cruziana
Palimpsest Softground
Low diversity Cruziana
Mixed Skolithos / Cruziana
Distal Skolithos
FS
SB/TSE
Transgressive Sandsheet
Offshore Transition
Upper Offshore
Lower Offshore
TSE
Estuarine Channel
SB/FS
SB/FS/TSE
Transgressive Sandsheet
Toxic Estuarine Billabong
Marine Influenced Estuarine Basin
Lower Offshore
Transgressive Sandsheet
Lower Shoreface Equivalent
Middle Shoreface Equivalent
Wave Dominated Delta Front
Proximal Lower Shoreface Equivalent
Estuarine Basin
Upper Offshore
Lower Offshore
n=5
n=38
n=30
n=22
n=47
n=14
n=44
n=29
Estuarine Channel (IHS Lateral Accretion Deposits)
Low diversity Cruziana
Abandoned Estuarine Billabong
Bi
mud
silt
v.f.sand
f.sand
m.sand
c.sand
v.c.sand
gran.
conglom.

Figure 15

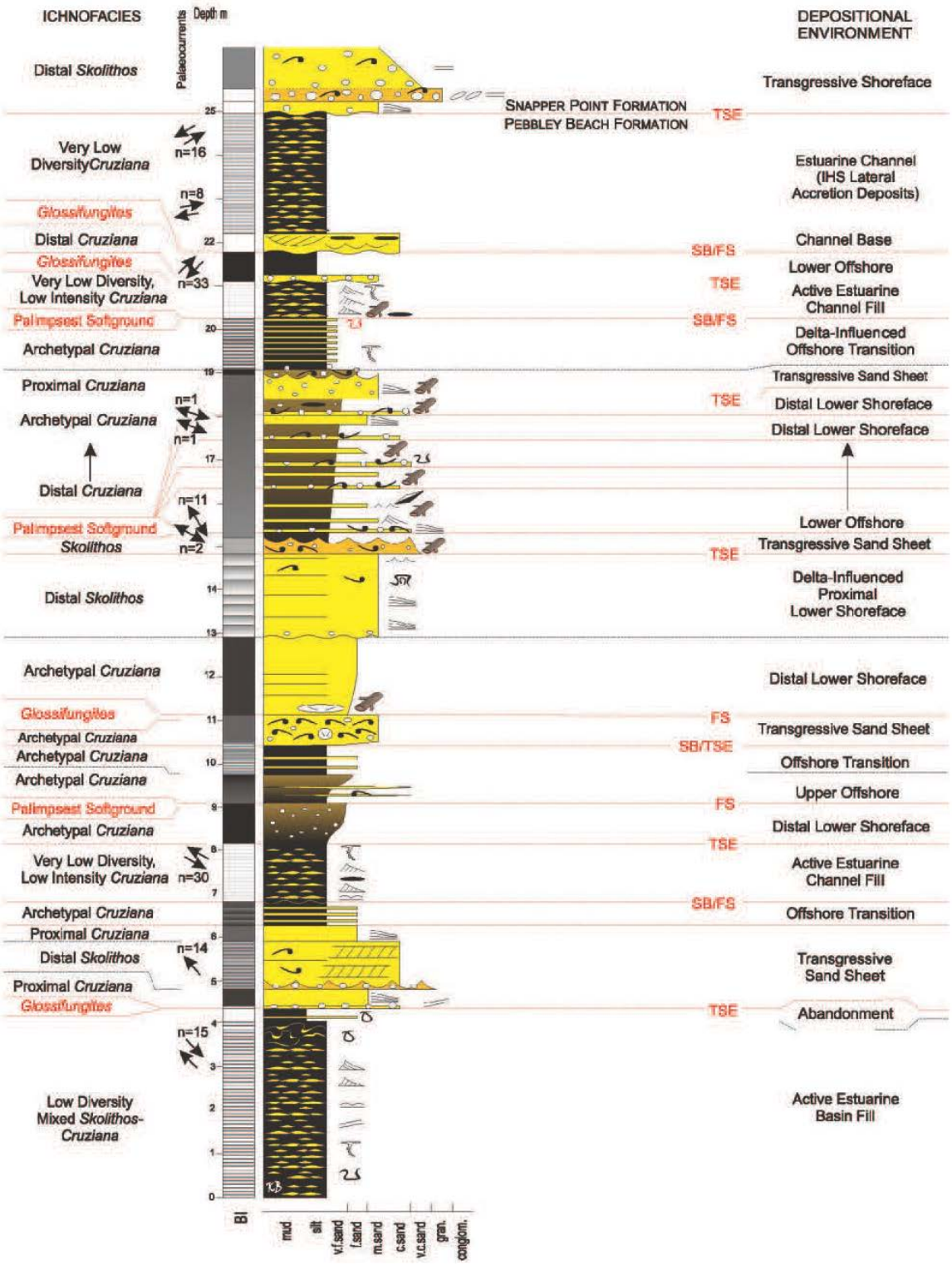
ICHNOFACIES
Depth m
Palaeocurrents
DEPOSITIONAL ENVIRONMENT
Distal Skolithos
Transgressive Shoreface
SNAPPER POINT FORMATION
PEBBLEY BEACH FORMATION
TSE
Very Low DiversityCruziana
n=16
Estuarine Channel (IHS Lateral Accretion Deposits)
n=8
Glossifungites
Distal Cruziana
Channel Base
SB/FS
Glossifungites
Lower Offshore
Very Low Diversity, Low Intensity Cruziana
n=33
TSE
Active Estuarine Channel Fill
Palimpsest Softgrounc
SB/FS
Archetypal Cruziana
Delta-Influenced Offshore Transition
Transgressive Sand Sheet
Proximal Cruziana
TSE
Distal Lower Shoreface
Archetypal Cruziana
n=1
n=1
Distal Lower Shoreface
Distal Cruziana
n=11
Lower Offshore Transgressive Sand Sheet
Palimpsest Softgrounc
Skolithos
n=2
TSE
Distal Skolithos
Delta-Influenced Proximal Lower Shoreface
Archetypal Cruziana
Distal Lower Shoreface
Glossifungites
FS
Transgressive Sand Sheet
Archetypal Cruziana
SB/TSE
Archetypal Cruziana
Offshore Transition
Archetypal Cruziana
Upper Offshore
Palimpsest Softgrounc
FS
Archetypal Cruziana
Distal Lower Shoreface
TSE
Very Low Diversity, Low Intensity Cruziana
n=30
Active Estuarine Channel Fill
Archetypal Cruziana
SB/FS
Offshore Transition
Proximal Cruziana
Distal Skolithos
n=14
Transgressive Sand Sheet
Proximal Cruziana
Glossifungites
TSE
Abandonment
n=15
Low Diversity Mixed Skolithos-Cruziana
Active Estuarine Basin Fill
BI
mud
silt
v.f.sand
f.sand
m.sand
c.sand
v.c.sand
gran.
conglom.

Figure 16

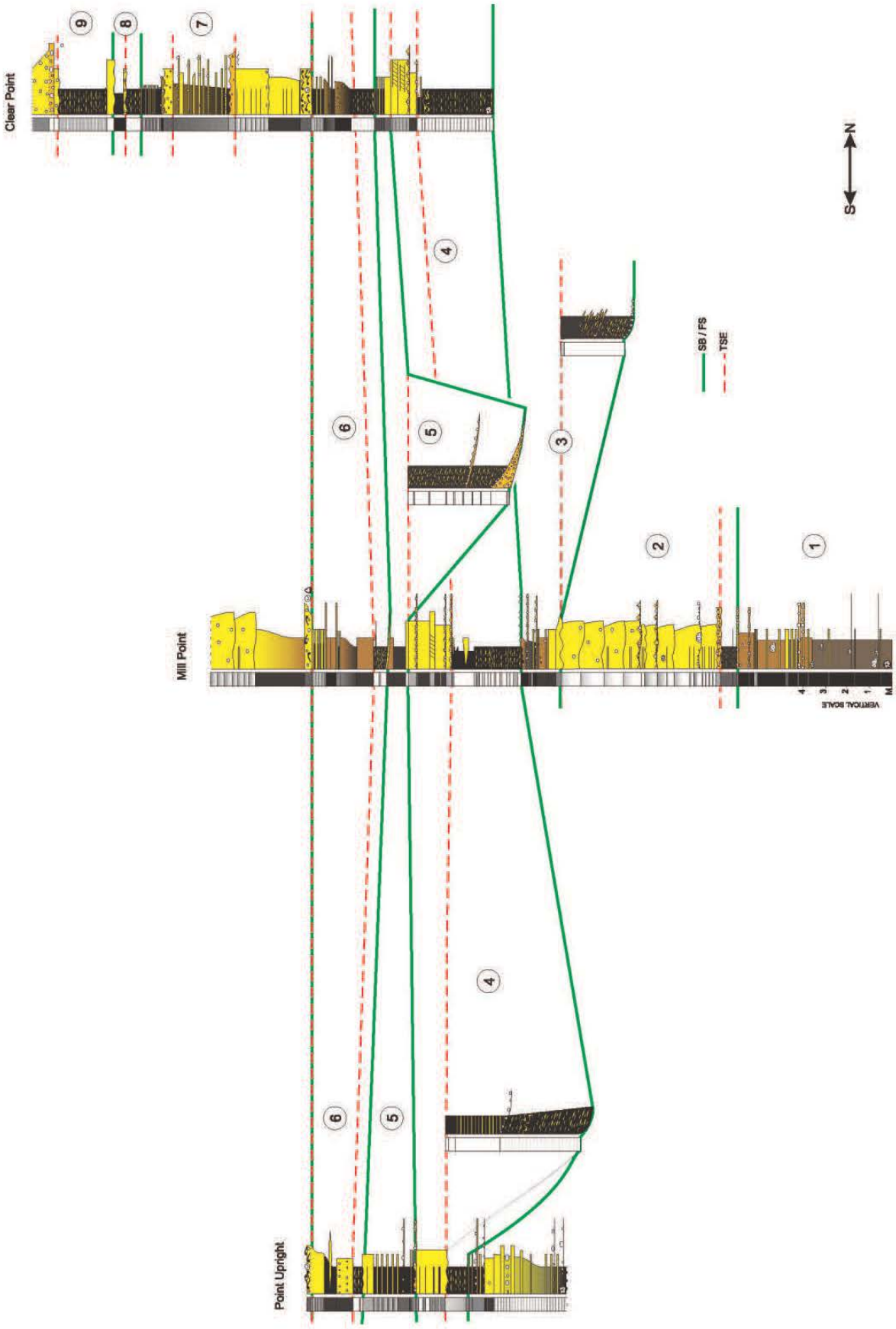
Clear Point
Mill Point
Point Upright
9
8
7
6
5
4
3
2
1
SB / FS
TSE
S
N
VERTICAL SCALE

Figure 17

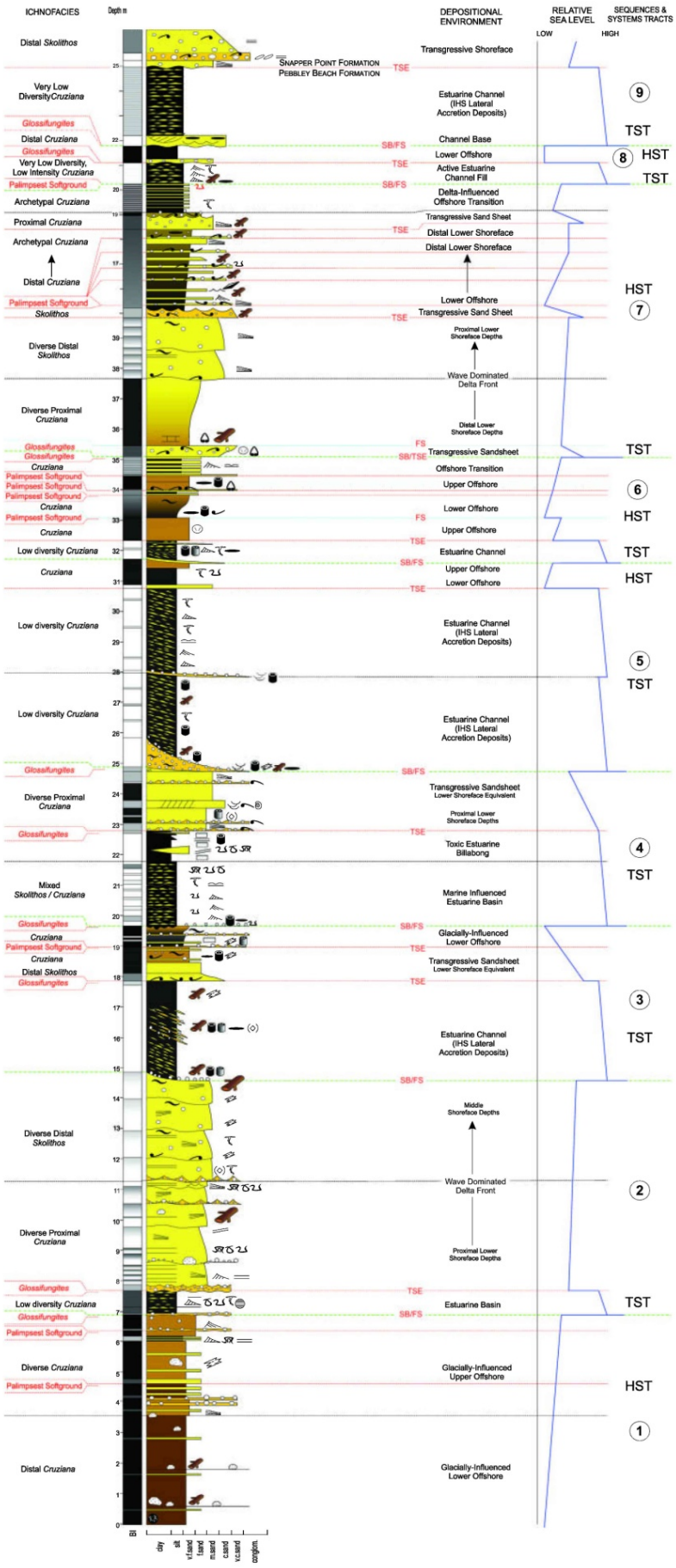
ICHNOFACIES
Depth m
DEPOSITIONAL ENVIRONMENT
RELATIVE SEA LEVEL
LOW
HIGH
SEQUENCES & SYSTEMS TRACTS
Distal Skolithos
Snapper Point Formation
Pebbley Beach Formation
Transgressive Shoreface
TSE
Very Low Diversity Cruziana
Glossifungites
Distal Cruziana
Glossifungites
Estuarine Channel (IHS Lateral Accretion Deposits)
9
TST
Channel Base
SB/FS
Lower Offshore
8
HST
Very Low Diversity, Low Intensity Cruziana
Palimpsest Softground
TSE
Active Estuarine Channel Fill
TST
SB/FS
Archetypal Cruziana
Delta-Influenced Offshore Transition
Proximal Cruziana
Transgressive Sand Sheet
TSE
Archetypal Cruziana
Distal Lower Shoreface
Distal Lower Shoreface
Distal Cruziana
Palimpsest Softground
Skolithos
Lower Offshore
HST
Transgressive Sand Sheet
TSE
7
Diverse Distal Skolithos
Proximal Lower Shoreface Depths
Wave Dominated Delta Front
Diverse Proximal Cruziana
Distal Lower Shoreface Depths
Glossifungites
Glossifungites
Cruziana
FS
SB/TSE
Transgressive Sandsheet
TST
Palimpsest Softground
Palimpsest Softground
Palimpsest Softground
Offshore Transition
Upper Offshore
6
Cruziana
Palimpsest Softground
Lower Offshore
FS
HST
Cruziana
Upper Offshore
TSE
Low diversity Cruziana
Estuarine Channel
TST
SB/FS
Cruziana
Upper Offshore
HST
Lower Offshore
TSE
Low diversity Cruziana
Estuarine Channel (IHS Lateral Accretion Deposits)
5
TST
Low diversity Cruziana
Estuarine Channel (IHS Lateral Accretion Deposits)
Glossifungites
SB/FS
Transgressive Sandsheet
Lower Shoreface Equivalent
Diverse Proximal Cruziana
Proximal Lower Shoreface Depths
Glossifungites
TSE
Toxic Estuarine Billabong
4
TST
Mixed Skolithos / Cruziana
Marine Influenced Estuarine Basin
Glossifungites
SB/FS
Cruziana
Glacially-Influenced Lower Offshore
Palimpsest Softground
TSE
Cruziana
Transgressive Sandsheet
Lower Shoreface Equivalent
Distal Skolithos
Glossifungites
TSE
3
Estuarine Channel (IHS Lateral Accretion Deposits)
TST
SB/FS
Middle Shoreface Depths
Diverse Distal Skolithos
Wave Dominated Delta Front
2
Diverse Proximal Cruziana
Proximal Lower Shoreface Depths
Glossifungites
TSE
Low diversity Cruziana
Estuarine Basin
TST
Glossifungites
SB/FS
Palimpsest Softground
Diverse Cruziana
Glacially-Influenced Upper Offshore
Palimpsest Softground
HST
1
Distal Cruziana
Glacially-Influenced Lower Offshore
BS
clay
silt
v.f.sand
f.sand
m.sand
c.sand
v.c.sand
conglom.

Figure 18